Characterization of Maturation of Tissue Engineered Skeletal Muscle Bundles in Rheumatoid Arthritis

by

Hailee Bharat Patel

Department of Biomedical Engineering
Duke University

Date: _____

Approved:

_____
George Truskey, Chair

_____
Nenad Bursac, Advisor

_____
Shyni Varghese

Thesis submitted in partial fulfillment of
the requirements for the degree of Master of Science in the Department of
Biomedical Engineering in the Graduate School
of Duke University

2019

ABSTRACT

Characterization of Maturation of Tissue Engineered Skeletal Muscle Bundles in Rheumatoid Arthritis

by

Hailee Bharat Patel

Department of Biomedical Engineering
Duke University

Date: _____

Approved:

_____
George Truskey, Chair

_____
Nenad Bursac, Advisor

_____
Shyni Verghese

An abstract of a thesis submitted in partial fulfillment of the requirements for the degree of Master of Science in the Department of Biomedical Engineering in the Graduate School of Duke University

2019

Abstract

Rheumatoid Arthritis (RA) is a chronic inflammatory auto-immune disease typically involving the joints, mainly the diarthrodial joint and generally starts between the age of 30 and 60 in women and somewhat later in life in men. It is the most common inflammatory arthritis and about one percent of the population is affected by RA. A complex interaction between various genetic and environmental factors lead to the development of the disease, though the specific cause of RA is not known. The goal of this study is to characterize the maturation of skeletal muscle bundles made with myoblasts isolated from RA patients and compare it with maturation of age-matched controls. Moreover, the engineered myobundles were treated with pro-inflammatory cytokines to assess their effect on the bundle maturation and to replicate the pro-inflammatory phenotype of RA.

Myobundles were prepared with human skeletal muscle (HSkM) samples obtained from young controls, age-matched controls and RA patients through biopsy of vastus lateralis muscle (biopsy of hamstring muscle was taken for young controls). We measured nuclei count, cross-sectional area, Myogenin count, Sarcomeric alpha-actinin (SAA) positive area and the myofiber diameter for each time course studies and cytokine treated bundles.

Contrary to our expectations, the time course study did not indicate significant reduction in fiber formation. This may be due to the effect of medications taken by the RA patient which might be helping the muscle function. Another possible reason might be that the cells could have regained their normal function once they were taken out from the inflammatory environment induced by the pro-inflammatory cytokines. Yet another possible reason may be that the time

course considered may not be enough to access changes in the maturation and a longer time period may be required.

We then moved forward to replicate the disease pro-inflammatory phenotype by carrying out cytokine treatments on the engineered myobundles. IFNγ, IFNγ+GMCSF, TNFα+GMCSF and IFNγ+TNFα+GMCSF were chosen for the cytokine treatments. According to our results, the cross-sectional area, nuclei count/CSA, MyoG count/CSA, MyoG/Nuclei count, SAA+ area and the myofiber diameter each decreased with cytokine treatments indicating that the cytokines may indeed affect the regeneration ability of skeletal muscle cells.

The results from cytokines treatment studies indicate that cytokines do play a role in disease development and progression. A longer time course study say for up to 10 days or more post differentiation, more patient data regarding the disease severity and medications might also be helpful in further investigation.

Dedication

I dedicated this work to my dear family. They have always supported and encouraged me to move forward. They have always been curious of my work and have helped me in every way possible. Without their love, help and support, I would not have made it this far.

Contents

List of Tables

List of Figures

Acknowledgements

I would like to thank my supervisor, Dr. George Truskey for his mentorship and guidance during my study. I am grateful for his time, encouragement and attention to this project. I also thank Dr. Nenad Bursac for his valuable discussion and encouragement. I've truly enjoyed working on the project under their guidance.

I would also like to thank my graduate mentor Catherine Oliver for her support and guidance in lab. I also want to thank all the lab members of Truskey lab, all the fun events that we had apart from working in the lab were a great way to know everyone and take a break from our busy work lives. It was a great experience.

Lastly, I would like to thank all my friends at Duke with whom I've spent endless nights working and chatting with background music, though none of our fields are same. Thanks for the wonderful times, I'll always miss them, and these moments will always make me smile. You guys made graduate school at Duke a wonderful experience.

1. Introduction

1.1 Skeletal Muscle Physiology and Maturation

Skeletal muscle, a form of striated muscle tissue comprises over 40% of our body's total muscle mass and most are attached to bones by tendons at both ends. They are responsible for muscle contraction to move the bones across the joint under the control of somatic nervous system. Moreover, the skeletal muscle system is also important for regulating the calcium levels, producing cellular components of the blood, maintaining posture, joint stability, and internal heat production. Skeletal muscles can vary significantly in size, shape, and arrangement of fibers according to the location of the muscle to meet the physiological demand.

The structure of a skeletal muscle is shown in figure 1 below. In brief, skeletal muscle is composed of muscle fascicles (mm) which are surrounded by epimysium. The fascicles contain muscle fibers (μm x 100) running in parallel and surrounded by perimysium, a layer of connective tissues that house nerves and blood vessels. The parallel structure allows for the effective transmission of contraction and cumulative peak force generation. Each muscle fiber in turn is a collection of myofibrils (μm) joined together by endomysium. Each myofiber contain numerous mitochondria and are surrounded by many peripheral nuclei. Each myofibril consists of sarcomeres and is surrounded by sarcoplasmic reticulum [1].

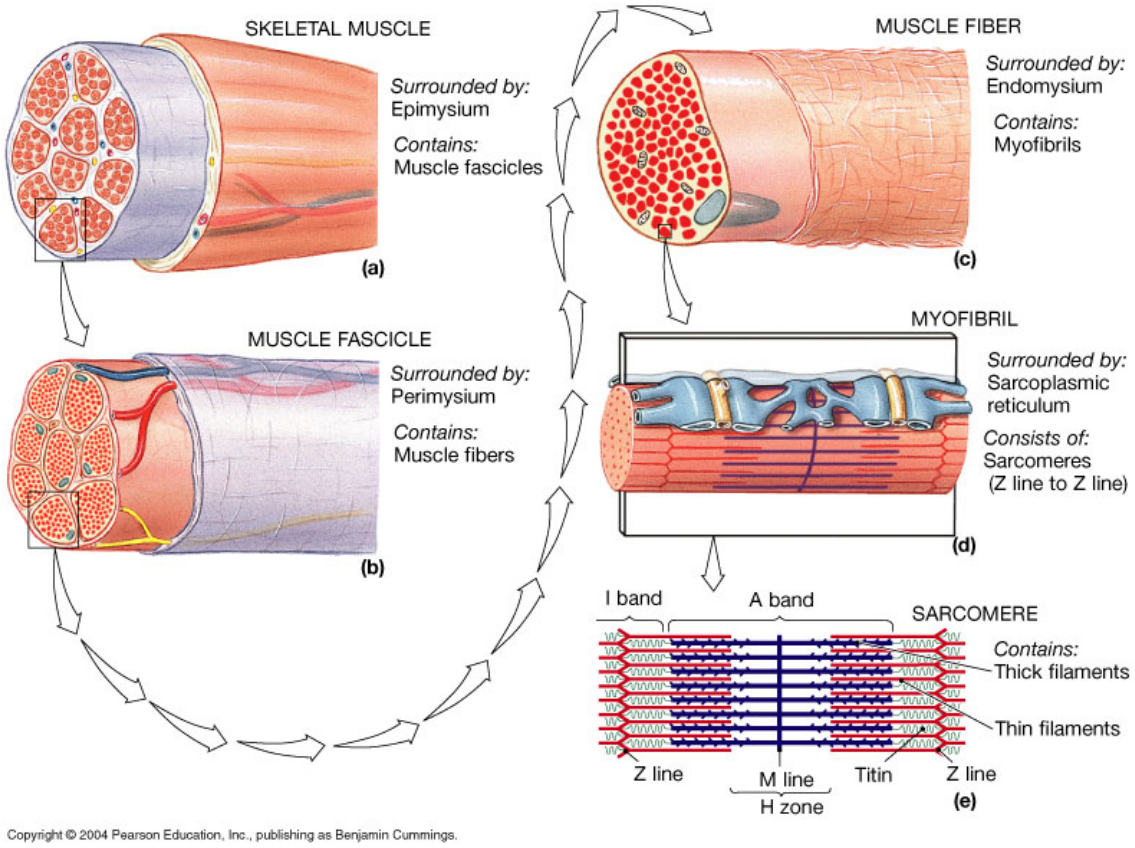

Figure 1: Structure of skeletal muscle [2]

A sarcomere, the basic contractile unit of muscle, is composed of myofibrillar proteins that allow muscle contraction, including actin (thin) and myosin (thick) filaments. The filaments interdigitate to form areas of overlap forming the A-band, M-band, I-band and Z-band, which lengthen and shorten with contraction. The heavy chains contain the myosin head that bind with actin and allow the muscles to contract. The thin filament is composed of actin and regulatory proteins troponin and tropomyosin. When a stimulus is received, calcium released from sarcoplasmic reticulum binds to troponin which causes tropomyosin to expose the myosin binding domain on the actin filament. In presence of ATP, the myosin head pulls the actin along the myosin providing the contraction. Each sarcomere is separated by Z-lines, where actin filaments

are anchored. The antiparallel dimers of sarcomeric alpha actinin (SAA) are responsible for anchoring the actin filaments from adjacent sarcomeres and stabilize them against the contractile forces. The structure of sarcomere is shown in figure 2 below.

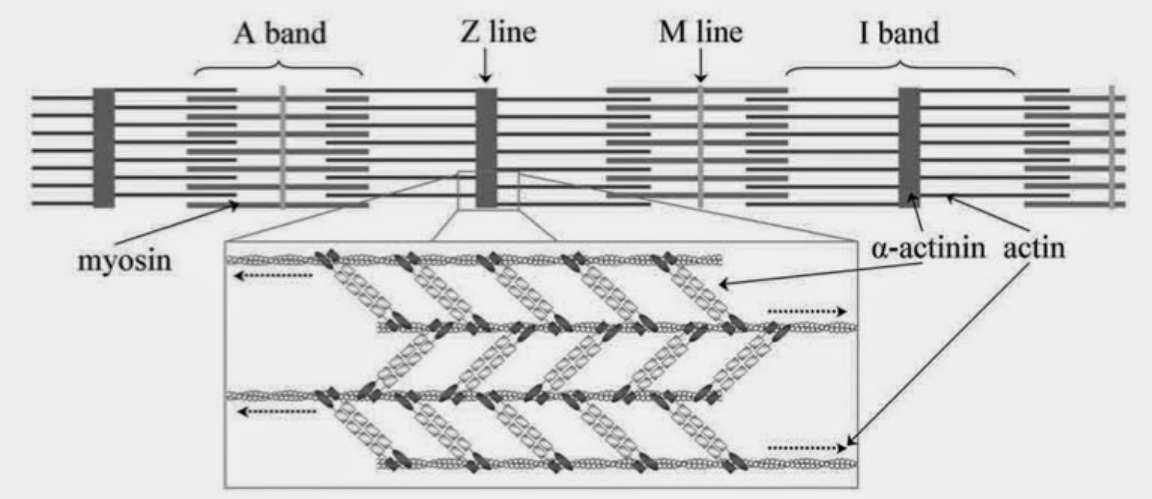

Figure 2: Structure of sarcomere [3]

The regenerative capacity of skeletal muscle fibers depends on the pool of undifferentiated myogenic progenitor cells called the satellite cells which are present between the basal lamina and sarcolemma [4]. The satellite cells remain quiescent under normal conditions in the periphery of the myofibers and exhibit limited gene expression and protein synthesis [5]. After damage to myofibers, activation cues released from the myofibers signal satellite cells to leave the basal lamina, where they begin to proliferate. CD34 and Pax7 are expressed during the change from quiescent to activated stage in the satellite cells [6]. These activated satellite cells are known as myoblast, which are mononucleated and proliferative and they express MyoD and MRF5 [7]. As the myoblast exit cell cycle and enter the terminal differentiation stage, myogenin and MRF4 are up-regulated to promote muscle differentiation. Myogenin is specifically responsible for

fusion and formation of myofibers or myotubes, while MRF4 plays a role in muscle maturation [8,9]. These muscle cells then fuse and differentiate into myotubes and start expressing α-actinin and myosin heavy chains.

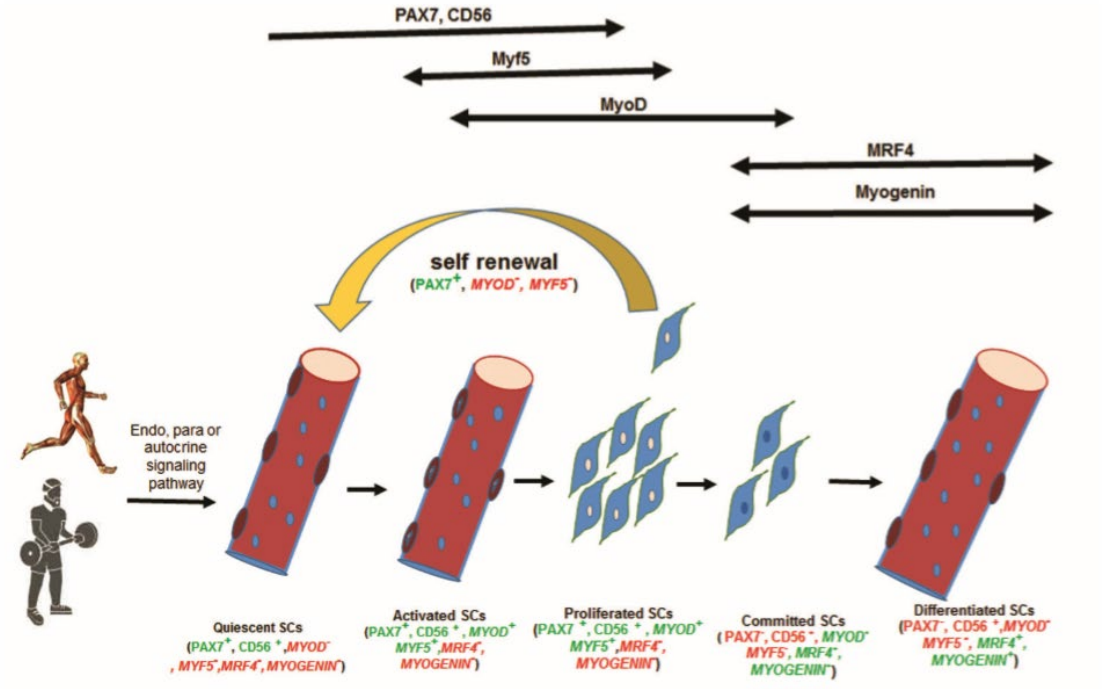

Figure 3: Morphological and Functional changes in satellite cells [10]

1.2 Rheumatoid Arthritis

Rheumatoid Arthritis (RA) is a chronic inflammatory auto-immune disease typically involving the joints, mainly the diarthrodial joint and generally starts between the age of 30 and 60 in women and somewhat later in life in men. It is the most common inflammatory arthritis and about one percent of the population is affected by RA [11] and the world burden is expected to rise. Out of every 100,000 people, 41 are diagnosed with RA every year and women are about two to three times more likely to get RA than men. Hormones in both genders may play a role in either

preventing or triggering it. RA can affect organs such as the heart, the lungs, eyes, skin, vascular system or other tissues like muscles, cartilage, and ligaments. Eventually, it may affect larger joints such as hips, shoulders and knees and may damage joints within three to six months of onset. Sixty percent of people with inadequately treated RA are unable to work 10 years after onset.

Figure 4: Prevalence of rheumatoid arthritis in the adult population of various world regions. [12]

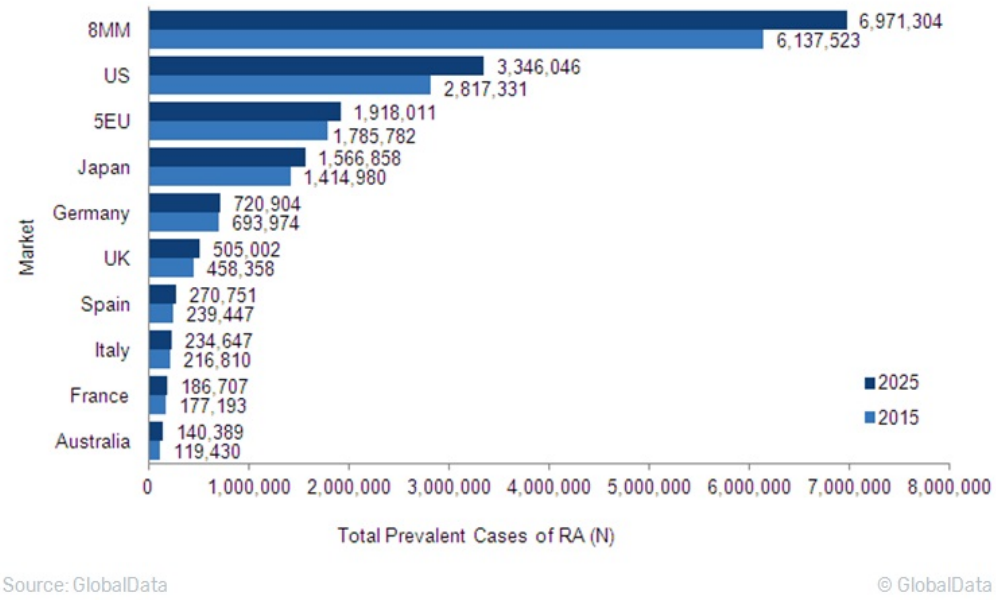

Figure 5: Global RA Prevalence [13]

A complex interaction between various genetic and environmental factors lead to the development of the disease, though the specific cause of RA is not known [14]. Human leukocyte antigen (HLA) major histocompatibility complex (MHC) genes clearly define the susceptibility to RA. Furthermore, many other genes including cytokine promoters and T cell signaling genes also contribute to susceptibility and severity. However, genes are not the sole influence, environmental stimuli such as smoking and epigenetic factors such as abnormal DNA or expression of microRNAs may also play a role [15]. Repeated activation of innate immunity caused by the environmental factors cause increased production of auto-antibodies like Rheumatoid factors (RF) and anti-citrullinated protein antibodies (ACPAs), type 2 collagen and IgG. This leads to increased synovial inflammation which subsequently leads to increase in vascular leakage and provides access to the synovial lining which permits complement fixation, recruitment of leucocytes and lymphocytes, inflammation as well as increased production of

inflammatory cytokines. Once the inflammatory process is fully established, it causes matrix and joint destruction, physical disability, degradation of bone and cartilage, muscle weakness as well as pain.

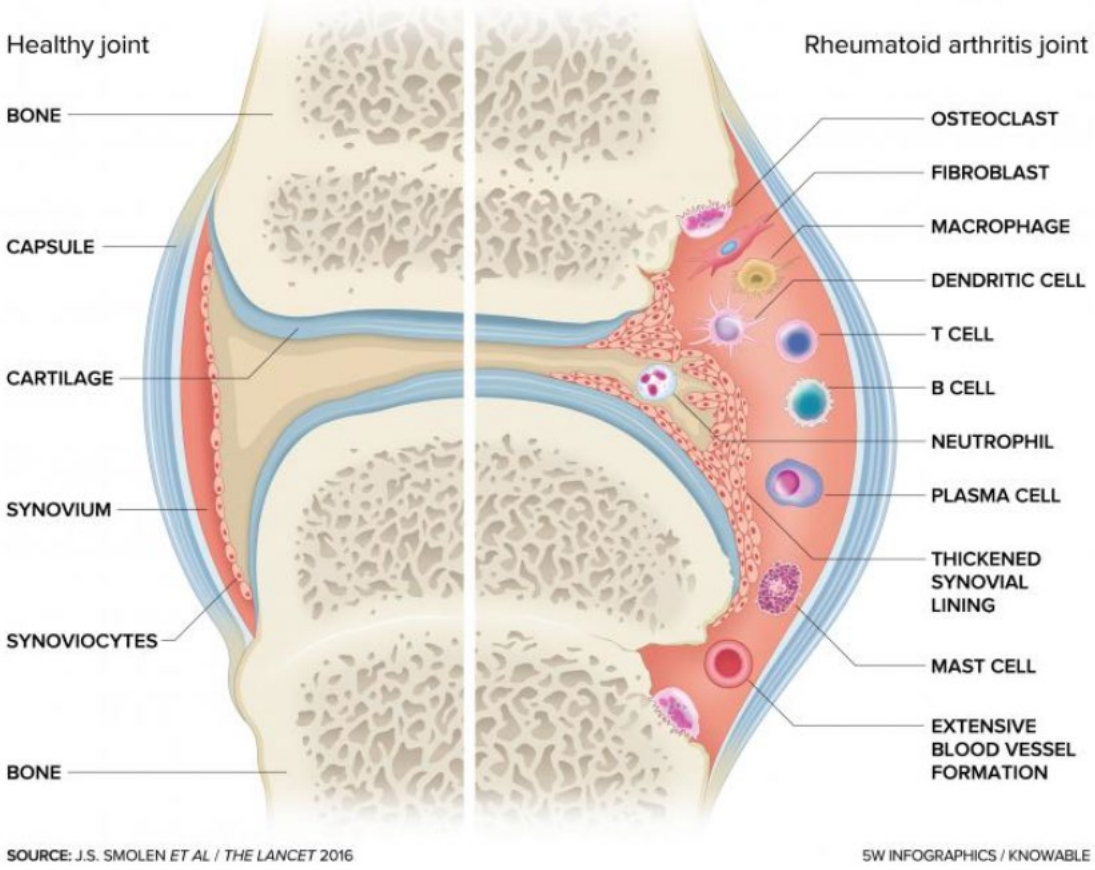

Figure 6: Anatomy of RA joint [16]

1.3 Cytokines involved in RA

Cytokines are small peptides (~5-20kDa) that are secreted by immune cells and include chemokines, interferons, interleukins, lymphokines and tumor necrosis factors. Cytokines are shown to be involved in cell to cell communication in immune response and stimulate the movement of cells toward the site of inflammation, infection and trauma. They act through

receptors and modulate the balance between humoral and cell-based immune responses. Furthermore, they also regulate the growth, maturation and responsiveness of particular cells. In RA, cytokines may be classified in to four groups namely pro-inflammatory cytokines, inflammatory cytokines in joints, anti-inflammatory cytokines and natural cytokine antagonists. Synovitis (inflammation) in joints results from differentiation of T cells into Th_{17} cells, B cells further the pathogenic process through cytokine and autoantibody production, and antigen production [17].

Proinflammatory cytokines and macrophages may play a key role in initiation and development of RA through autocrine and paracrine communications causing reduction in regeneration ability and force generation. In addition, they also promote the development of systemic effects, causing anemia, cardiovascular disease, fatigue and depression. A cascade network of cytokines is involved in RA, including granulocyte macrophage colony – stimulating factor (GM-CSF), interleukin (IL)-2, IL-15, IL-13, IL-17, IL-18, interferon-gamma (IFN γ), tumor necrosis factor-alpha (TNFα) and transforming growth factor-beta (TGFβ) [18]. The release of cytokines, especially TNFα, IL-6 and IL-1 cause synovial inflammation. Clinical results showed increased production of IL-6 in muscles of RA patients [19].

TNFα is a key cytokine which induces GM-CSF production by antigen presenting cells (APCs), enhances T-cell proliferation and differentiation of B-cells, induces expression of adhesion molecules on endothelium, generates expression of collagenase, stromelysin (matrix metalloproteinase-3), and prostaglandins by synovial cells [20] and may interfere with antigen specific and non-specific suppressive effects of regulatory T cells [21]. The administration of anti-TNF antibodies or a TNF receptor fusion protein decreases the activity of disease [22]. GM-CSF

activates expression of human leucocyte antigen (HLA)-DR molecules on the APCs, thereby initiating T cell activation in presence of antigen or superantigen [23]. Clinical trials have confirmed that blocking GM-CSF with monoclonal antibodies decreases disease severity in RA [24,25]. IFNγ generated by activated T cells are found in small quantities in rheumatic tissues and are responsible for immune modulation (protection and activation).

The early symptoms of RA may start with fatigue, slight fever, weight loss, stiffness and joint pain, swelling and redness. Though as the disease progresses, it can also affect the whole body. It may cause inflammation on the surface of the eyes and on the membrane surrounding the lungs. Heart can also be affected, resulting in inflammation around the heart and in the heart muscle. Moreover, infection may occur in the heart valves. Apart from the individual organs, nerves, blood and blood vessels also get affected by RA, causing decrease in white blood cells and red blood cells, spleen enlargement, open ulcers and atherosclerosis. There may be nerve compressions as well as loss of strength in muscles. Skeletal muscles undergo broad-ranging molecular alterations in RA including gene expressions and inflammatory signaling causing disruption in signaling, remodeling and metabolic reprogramming which ultimately leads to physical inactivity and disability. Hence, skeletal muscle dysfunction might play a major role in RA disease activity.

1.4 Three-Dimensional Muscle Tissue Engineering

Tissue engineering is fast becoming the preferred technique to replace or repair damaged tissues, while also being used in drug discovery. The prime focus is on regenerating the concerned tissue by controlled growth of required cells (taken from the

body) in scaffold made from a suitable biomaterial. Skeletal muscle being responsible for every voluntary action of our body, have been extensively researched over the last few years. Common primary muscle disorders include inflammatory myopathies which are characterized by inflammation and progressive weakening of the skeletal muscles causing pain and impairing muscle function. Hence, skeletal muscle engineering has been extensively researched over the past few decades.

It is important to reproduce a physiologically functioning skeletal muscle that replicates the structure and force production of a native skeletal muscle tissue to understand the disease development, progression and consequently drug development. Advances in cell culture have made it possible to grow not only 2D monolayers or muscle but also develop 3D Skeletal Muscle, often referred to as myobundles that more closely mimic the native skeletal muscle. These 3D engineered tissue constructs possess many important in-vivo features, including the structural organization, presence of striations and presence of key functional proteins found in mature muscle bundles. Moreover, these engineered tissues also respond to external electrical stimulus producing spontaneous twitch force through contractions, which are comparable to the native tissue. They also exhibit tetany and fatigue in response to constant stimulation and exhibit similar force-frequency and length-tension relationships as an in-vivo myofibers.

Recently, the bundles are also being conditioned by external mechanical stimulations so that the engineered 3D constructs more closely replicate the native tissues

both in function and morphology, since morphology also affects the muscle function. However, apart from the external conditions, cell source and isolation from the excised tissues and selection of appropriate scaffold for cell maturation also play a role in developing a functional skeletal muscle mimicking in-vivo muscle. Mostly, collagen and fibrin gels, Matrigel, decellularized muscles or synthetic polymers are used as a scaffold material and the cell sources include rat and mouse myoblast cell lines, human primary myoblasts being the most recently used source since they can mimic the key functions more closely.

Hence, 3D engineered muscle show a great promise towards regenerative medicine, disease modelling, and drug screening and development. However, they need to be developed efficiently and the culture conditions properly maintained for them to be utilized for a relevant clinical outcome.

1.5 Goals

The goal of this study is to evaluate the muscle characteristics, evaluate the patients and further understand the underlying disease mechanism by characterizing myobundles made with cells from RA patients, more specifically to replicate the disease pro-inflammatory phenotype by cytokine treatments on tissue engineered myobundles and characterize the same for specific traits of RA. The bundles were treated with varying doses and combinations of TNFα, IFNγ and GM-CSF for the cytokine studies.

2. Methods and Materials

2.1 Isolation of Myogenic Satellite cells

Human skeletal muscle (HSkM) samples were obtained from young controls, age-matched controls and RA patients through biopsy of vastus lateralis muscle (hamstring muscle biopsies were considered for young controls) as per the Duke University Investigational Review Board approved protocols. Table 1 below shows the donors considered for our entire study and their information. The biopsy sample were placed in chilled solution of 50:1 Ca^{++} and Mg^{++} free Dulbecco's phosphate-buffered saline (**DPBS** -/-) and Antibiotic-Antimycotic (AA 100x), following which they were washed 3x with PBS+AA for 5 minutes each. The samples were then minced in a plastic petri dish using two sterile scalpels by pulling the fibers apart and split into groups of 0.5-1g each, which were placed into individual falcon tubes containing PBS+AA. Any floating fats and excess fluids were removed by washing 3-5 times. A solution of warm 0.05% trypsin was added to each tube and placed in a water-bath with periodic shaking for 30 minutes. The trypsin was deactivated with the addition of warmed hSkM growth media containing low glucose DMEM(Gibco), 8% heat-inactivated fetal bovine serum (Hyclone), 0.4µL Dexamethasone (Sigma), 10ng/mL EGF (VWR), 50ug/mL Fetuin (Sigma), 0.1% Gentamycin 1X (Gibco) and 0.1% Amphotericin B 1X, 1.5mg/mL ACA and filtered. The muscle tissues were plated onto uncoated T25 flask to remove undesired cells (fibroblasts, blood cells, nerve cells, etc.) by adhesion to plastic and incubated at 37°C for 2 hours, after which the tissues and media were transferred to Matrigel coated flask. The growth media was changed at days 2 and 5 after plating, followed by which the media was changed every other day until they cells were confluent. The cells were passaged 1:2 and trypsinized with 0.05% trypsin. After the cells were passaged the media was changed every other day until they reached full confluency. The cells

were then frozen down in media containing 90% growth media and 10%DMSO, at 1-2 million cells per mL.

Table 1: Donor information

Donor	Age	Gender
RAMC100b	55	F
RAMC101	62	F
RAMC104	65	F
RAMC105	61	F
RAE105	57	F
RAE109	59	F
RAME100	68	M
RAME101	61	M
RAME106	69	F

2.2 Thawing hSkM cells

GFR Matrigel (Corning) was thawed in the refrigerator overnight before using. 80 µL of GFR Matrigel was added to 16 mL of low glucose DMEM. 8 mL of Matrigel solution each was added to two T-175 flasks. The flasks were placed in incubator for 30 minutes to coat the flasks. The vial of cells was removed from -80°C freezer or liquid nitrogen and placed in water bath for 1-2 minutes until there was a bit of ice remaining. The cells were removed from the vial and added dropwise to 7mL of warmed hGM. The vial was washed with 1mL of hGM solution from the 7mL and added back to the cell suspension. The cell solution was centrifuged at 1000rpm for 5 minutes. The Matrigel solution was aspirated from flask and 20mL of hGM added to each flask.

The cell pellet was resuspended in 10mL hGM and 5mL added to each flask. The cells were distributed evenly by gently rocking from side to side.

2.3 Passaging hSkM cells

New T-125 flask were coated with 8ml of Matrigel solution prepared by taking 5 µl of Matrigel in 1mL of low glucose DMEM before bringing the cells. The flasks were placed in incubator for at least 30 minutes. The media was aspirated out from the side of the flask. Any remaining media was diluted with PBS without calcium/Magnesium and aspirated. 0.025% Trypsin/EDTA was added to the flask to detach the cells, the flask was allowed to stay in the incubator for 3-5 minutes to allow the cells to detach completely. If the cells did not detach, the sides of the flask were gently tapped to help them detach. The cells solution was transferred to an equal volume of warm solution of human growth media(hGM) to deactivate the trypsin. The number of cells were counted with a hemocytometer under a microscope. The cell solution was centrifuged at 1000rpm for 5 minutes. While the cells were spinning, the flasks were prepared by aspirating off the Matrigel solution and adding 20mL of growth media to each flask. Once the cells were done spinning, the supernatant was discarded, and the cell pellet resuspended in the appropriate amount of media (5mL for every flask) to form a single cell suspension. 5 mL of cell suspension was added to each flask and rocked gently to get an even cell suspension. The flasks were placed in incubator for the cells to become confluent again. Cells from each donor were passaged for 5 times (4 days) before differentiation in shift media containing low glucose DMEM (Gibco), 2% Horse Serum (Hyclone), 0.1% Gentamycin 1X (Gibco), 0.1% Amphotericin B 1X (Gibco), 10nM Insulin (Sigma) and 2.0 mg/mL 6-Aminocaproic Acid (ACA). Differentiation

media was changed every other day starting day 1 post-differentiation.

2.4 Bundle preparation

2.4.1 Fabrication of PDMS molds and Cerex frames

Polydimethylsiloxane (PDMS) (Dow Corning) was mixed in a ratio of 10 parts base elastomer to 1-part curing agent. The mixture was stirred with a pipette tip and placed in a desiccator to remove air bubbles for 30 minutes. The degassed PDMS mixture was poured over Teflon masters placed in a petri dish and air bubbles removed. The petri dish was placed in an oven to cure at 60-80°C for 4-6 hours, or until the PDMS is hardened. Once the PDMS is cured, PDMS block was removed from the petri dish and Teflon master were carefully removed to create a negative of the masters. The PDMS molds were then cut using a razor blade to create a small square containing the bundle reservoir area, retaining the flat surrounding area around the reservoir to pin the frames. The Cerex frames of size 1cm x 1cm were laser cut from a large Cerex fabric sheet.

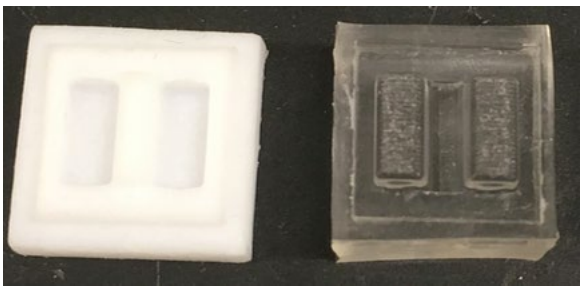

Figure 7: Teflon master (left) and corresponding PDMS negative molds

2.4.2 Sterilizing molds and frames

The molds were sterilized by sonicating for 45 minutes in 70% ethanol. Following which they were washed with PBS overnight and autoclaved for 20 minutes on gravity cycle in sealable autoclave pouches (12 molds per pouch).

Pins (Minutien Pins, Fisher Scientific) were inserted into frames made from PBN II 4.0 fabric (Cerex Advanced Fabrics, Inc.) through a corner of the frame and soaked in ethanol for at least 1 hour. After ethanol was removed, the flames were kept under UV overnight.

After sterilization, the molds were placed into 12-well plates using sterile forceps and soaked in 0.2% Pluronic (Sigma- Aldrich) solution for 30 minutes at room temperature. The molds were allowed to sit in sterile water (Gibco) for 30 minutes and dried. The Pluronic and water treatment prevents the myobundle from sticking to the PDMS mold by creating a hydrophobic surface on the mold. Once the frames are dried, they were pinned into the molds using sterile forceps.

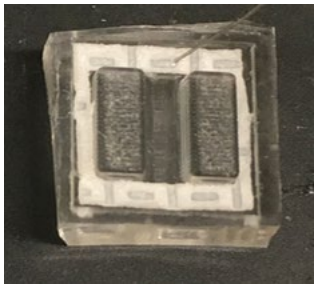

Figure 8: Cerex frames pinned into PDMS mold

2.4.3 Fabrication of Human Tissue Engineered Myobundles

The myobundles were prepare by encapsulating hSkM cell in a Matrigel/fibrin matrix and pipetted into the molds. A solution of 20 mg/mL fibrinogen (Sigma-Aldrich) was prepared by resuspending fibrinogen in warmed muscle growth media. The fibrinogen was sterile filtered using a syringe and syringe filter. The filtered fibrinogen solution was kept on ice until used. Cells were passaged normally by washing with PBS and adding 0.025% trypsin. The cells were counted and centrifuged at 1000rpm for 5 mins. After centrifuging, the pellet was resuspended in appropriate amount of cold growth media and placed on ice. Thrombin (Sigma-Aldrich) was added to cell solution. The thrombin/cell solution was mixed with Matrigel/growth media/fibrinogen and kept on ice. 50µL of the bundle solution was added to each mold, pipetting most of the volume into the center of the mold, and using the remaining solution to bring the middle volume in contact with the sides of the frames. The finished bundles were placed in incubator for 25-30 minutes, after which 3mL of warm growth media +ACA was added to each bundle. ACA was used to minimize the degradation of extracellular matrix of the myobundles. After 4 days, the media was changed to a differentiation media (shift media) supplemented with horse serum and the media was changed every other day. For time course studies, the myobundles were fixed at days 1,3 and 7 post-differentiation. For cytokine studies, the bundles were differentiated in serum free shift media (Low- glucose DMEM, N2 supplement, AA, ACA) and starting day 7 post-differentiation, the bundle were treated with either 10ng/ml GM-CSF or 20ng/ml IFNγ or 20 ng/mL IFN-γ + 10 ng/ml GM-CSF or 40 ng/mL TNF-α + 10 ng/ml GM-CSF or 40 ng/mL TNF-α + 20 ng/mL IFNγ + 10 ng/ml GM-CSF. The myobundles were fixed 10 days-post differentiation.

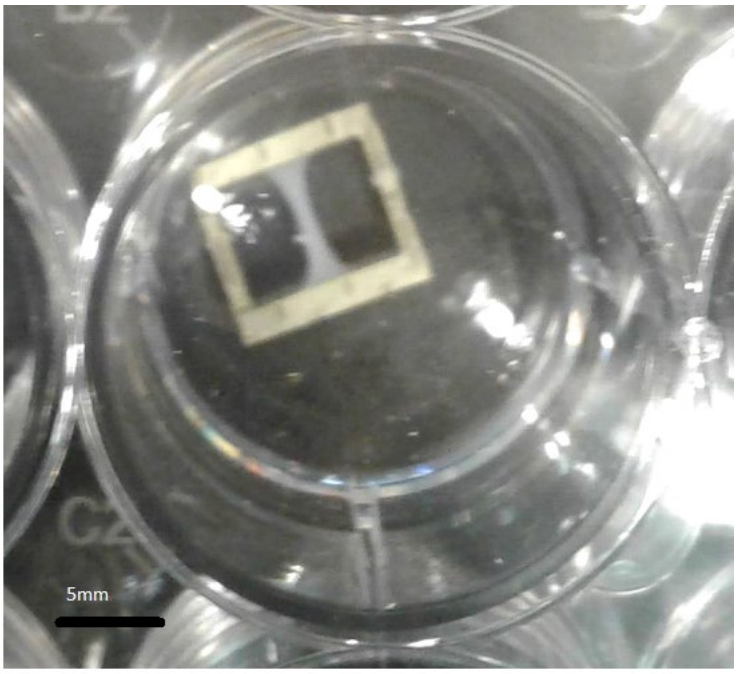

Figure 9: Cultured myobundle attached to Cerex frames

2.5 Fixing of myobundles

For time course studies, the myobundles were fixed at 1,3- and 7-days post-differentiation with 2% Paraformaldehyde (PFA) (Alfa Aesar) made in PBS+/+. While for cytokine studies, the myobundles were fixed at 10 days post-differentiation.

In brief the procedure used was as follows. The cultured myobundles were washed with PBS-/- for 5 minutes followed by which 1.5mL of 2% PFA was added to each bundle. The bundles were allowed to stay in PFA for 16-18 hours with shaking after which they were washed 3 times in PBS-/- for 5 minutes each. They were stored at 4°C until frozen in liquid nitrogen.

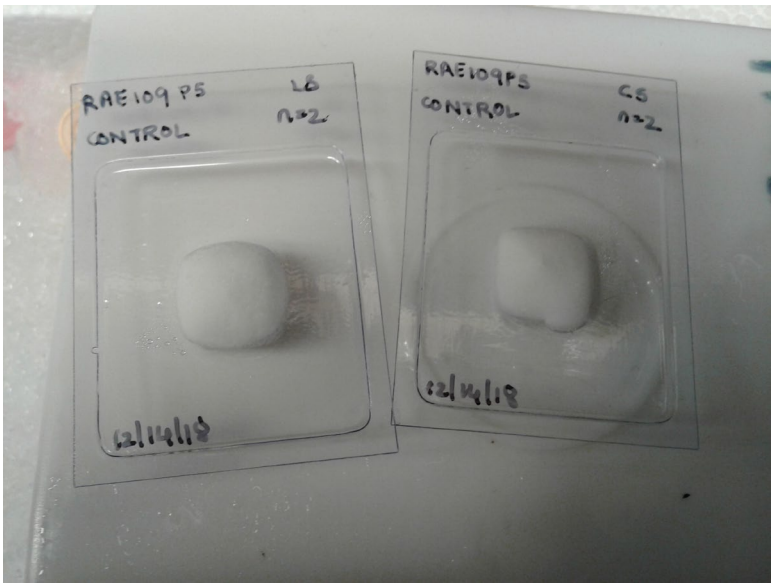

Figure 10: Myobundles frozen in OCT solution

2.6 Staining

All cross-sections of myobundles were stained for sarcomeric α-actinin (SAA) (1:250, Sigma), Myogenin (MyoG) (1:250, Abcam) and nuclei (1:1000, Hoechst 33342, Invitrogen). Each slide of the muscle bundle sections was washed three times with 1mL PBS for 5 minutes each. Hydrophobic pen was used to trace around samples and the samples permeabilized with 1mL 0.1% Triton-X for 30 minutes at room temperature. The samples were washed 2 times with 1mL PBS for 5 minutes each and incubated in blocking buffer (BB) for at least 2 hours at 4°C. BB was prepared by taking 1% Bovine Serum Albumin (BSA) (Sigma), 10% Goat Serum or Horse Serum (Thermo Fisher) in PBS. After 2 hours, primary antibodies (Anti-SAA mouse, Anti-MyoG rabbit) diluted 1:250 in BB were added to the samples and incubated overnight at 4°C. The samples were washed 3 times with 1mL BB for 10 minutes each. Followed by which filtered secondary antibodies (Alexa Fluor- 488 goat anti-Mouse Ab 1:250 Invitrogen, Alexa Fluor -633

goat anti-Rabbit Ab 1:250 Invitrogen, Hoechst) diluted in BB were added to the samples and incubated for 2 hours at room temperature. The secondary antibodies were removed by 3 washed of PBS for 10 minutes each. The slides were mounted under micro cover glass coverslip of size 22*50mm (VWR) using fluoromount-G (Southern Biotech) and stored at 4°C for 3 days until they were ready for imaging. The prepared slides were imaged using Leica SP5 Inverted Confocal Microscope.

2.7 Image Analysis

The proportion of nuclei contained within α-actinin-positive fibers were calculated to find the rate of fusion during myoblast differentiation. The proportion of nuclei having MyoG were calculated to track the maturation of myoblast. All data is represented as mean ± standard error of mean (SEM). All image analysis was carried out through ImageJ. Each donor had at least 2 muscle bundles for each condition and each bundle had at least 4 section taken into consideration while calculating the mean.

2.7.1 Cross sectional area

Lif (Leica image format) experiment files were imported in ImageJ. Under the analyze tab the set measurements tab was selected. Area, area fraction and ferret diameter were selected from the dialog box that opened. Freestyle tool was used to draw around the overlayed cross-section and area measured by pressing Ctrl M. The area calculated by ImageJ was given in microns which was converted to mm^2 as required.

2.7.2 Nuclei Count

The channels were split in the imported image by going to color under image tab. The DAPI (blue channel) was selected. The nuclei count was determined by using the nucleus counter of the particle analysis plugins. The minimum threshold was set to 2 and the maximum threshold was set to 500. The count displayed were the nuclei count. In some images if required the background was removed by thresholding and manually adjusting the threshold.

2.7.3 MyoG Count

The DAPI (blue) channel was selected and converted to mask from the binary menu under the process tab. Following which Image Calculator was used to get an image of the mask and MyoG (red) channel. MyoG count was calculated from the resulting image by using the nucleus counter and keeping the minimum threshold value as 2 and maximum threshold value as 500. The mask took care of additional background in the images.

2.7.4 SAA positive area

The SAA+(green) channel was selected. It was converted to 8-bit image from the type menu under image tab. The image was then made binary from the binary menu under the process tab. Freestyle tool was used to draw around the edges of the binary cross-section image and area measured. The Area and %Area values were used to determine the SAA+ area and the units scaled appropriately from microns to mm^2.

2.7.5 Fiber Diameter

The 5x images were imported for calculating the fiber diameter. The SAA (green) channel was selected. Freestyle tool was used to draw around the edges of SAA+ fiber and the ferret value recorded. Th diameter was determined for about 40-60 fibers total using 4-6 images.

2.8 Statistical Analysis

Two-way univariant ANOVA was conducted using SPSS tool to examine the statistical significance of effect of time and donor on the cross-sectional area for the time course studies while the effect of treatment and donor were considered for cytokine treatment studies.

3. Results

3.1 Time course studies

For time course studies, the cross-sections of myobundles taken at Days 1,3 and 7 post-differentiation were analyzed using ImageJ for total cross-sectional area, nuclei count, MyoG count, SAA positive area and total fiber diameter. Each donor had at least 2 muscle bundles for each condition. A maximum of 4 bundles were considered for the analyses for each donor. Each of these bundles in turn had between 4 or 5 sections taken into consideration while calculating the mean. Table 2 summarizes the donors considered for time-course studies. The graphs below have all data represented as the mean ± standard deviation of mean

Table 2 : Donors characterized for time course studies

Young Donors	Age-matched Donors	RA Donors
T104 (3 bundles, 5 sections each)	RAMC100b (3 bundles, 5 sections each)	RAE105 (3 bundles, 5 sections each)
T105 (3 bundles, 5 sections each)	RAMC101 (3 bundles, 5 sections each)	RAE109 (3 bundles, 4 sections each)
T106 (4 bundles, 5 sections each)	RAMC104 (4 bundles, 5 sections each)	RAME100 (4 bundles, 5 sections each)
	RAMC105 (3 bundles, 5 sections each)	RAME101 (3 bundles, 5 sections each)

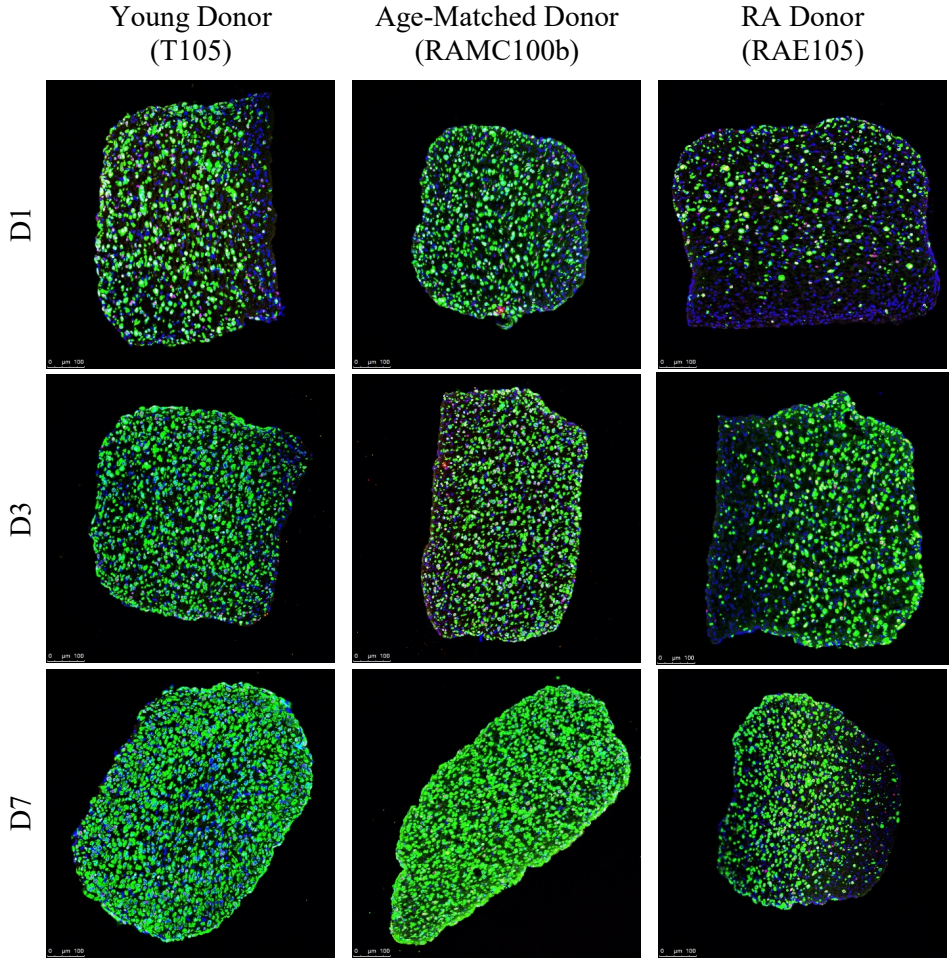

Figure 11: Cross-sections for each donor at days 1,3 and 7 post differentiation

3.1.1 Cross-sectional area

The cross-sectional area was calculated in microns from ImageJ. Figure 12 represents the average cross-sectional area calculated for each donor for days 1,3 and 7 post differentiation.

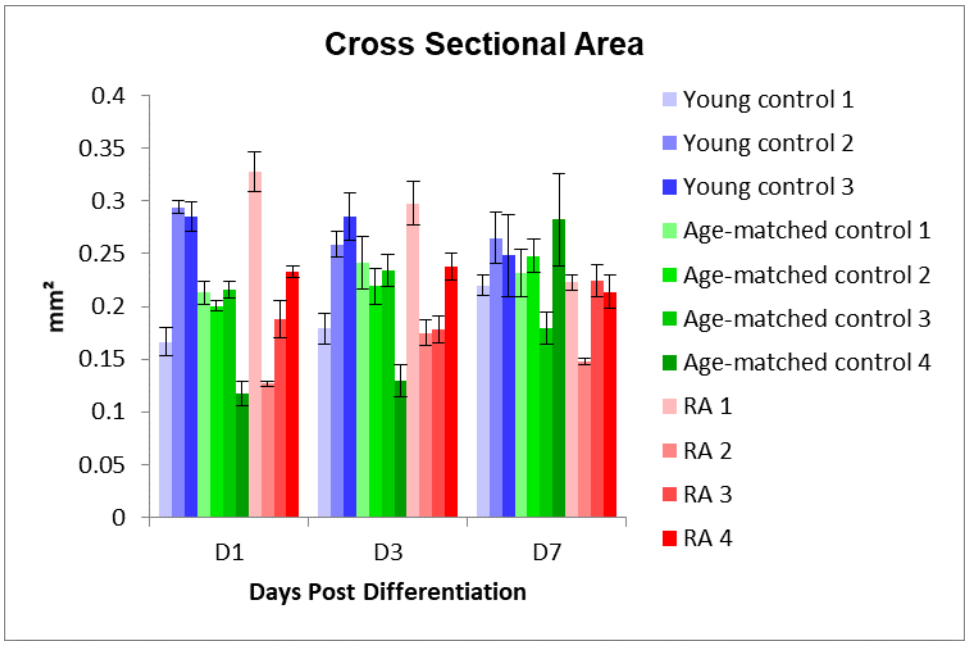

Figure 12 : Cross Sectional Area for time course studies

For better comparison, all the donors in one group were averaged together and the results are summarized in figure 13. The cross-sectional area of the myobundles from young donors remained almost the same, while for the age-matched controls the area increased slightly with time and for RA donors they decreased slightly from day 1 towards day 7.

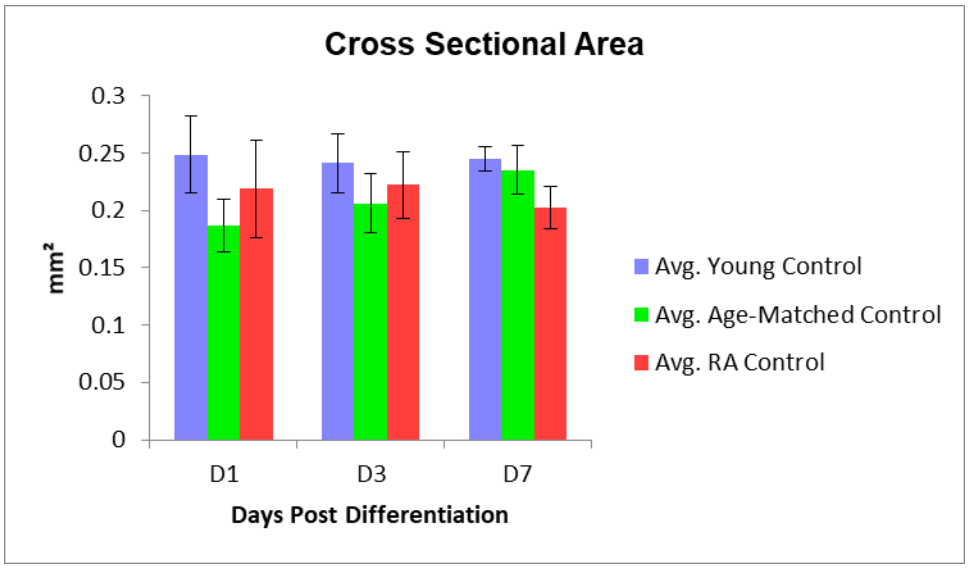

Figure 13 : Averaged CSA of myobundles for time course studies

A univariant two-way ANOVA was conducted using SPSS tool to examine the statistical significance of effect of time and donor group on the cross-sectional area. The results indicated that there were no statistically significant interactions between the donor groups and days-post differentiation on the cross-sectional area. The p-value for days was found to be 0.927, for donor group it was found to be 0.325 while for their interaction it was found to be 0.789 which were all greater than the significance level of 0.05 considered for the analysis.

3.1.2 Nuclei Count/Cross Sectional Area

The nuclei counts were calculated using the Nucleus Counter of the Particle Analysis Plugin of ImageJ. Nuclei counts were measured to access the number of cells in the bundle and see the effect of maturation on the same. For comparison between the donors the counts were normalized with the cross-sectional area of the respective bundles. Figure 14 represents the nuclei counts obtained for each donor.

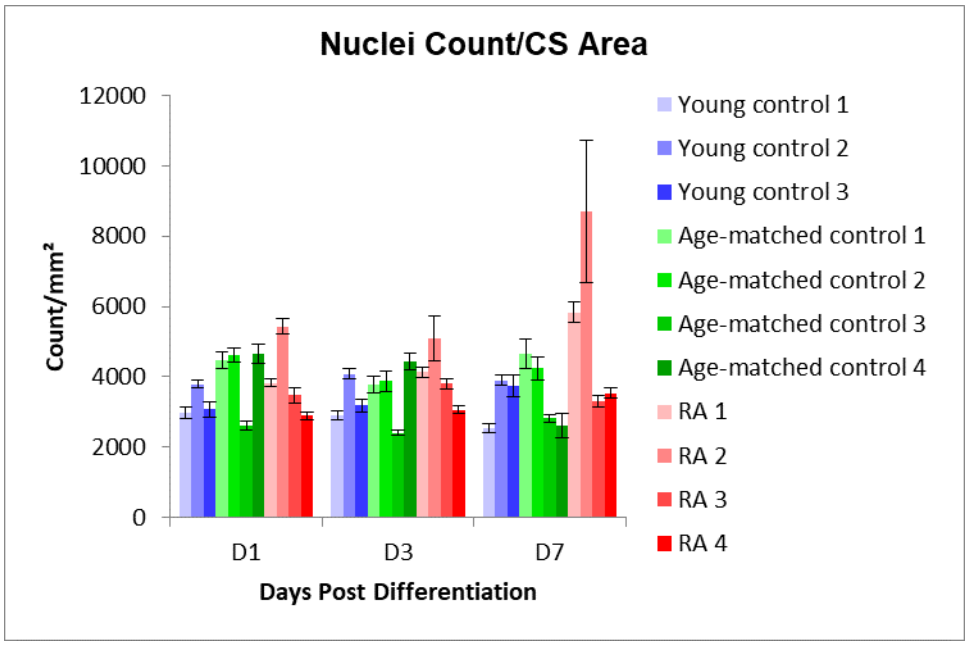

Figure 14: Nuclei Count/CSA of myobundle for time course studies

For better comparison, all the donors in one group were averaged together and the results are summarized in figure 15. The nuclei count/cross-sectional area increased with time for RA donors at day 7 post-differentiation while it decreased for age-matched controls and remained almost the same for young controls.

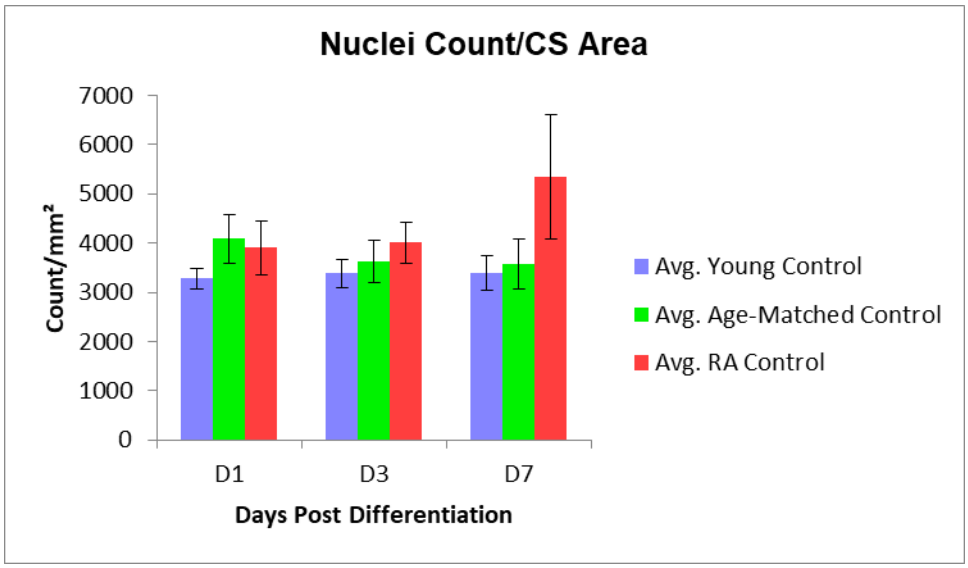

Figure 15: Averaged Nuclei Count/CSA of myobundles for time course studies

The two-way ANOVA results indicated that there were no statistically significant interactions between the donor groups and days-post differentiation on the nuclei count. The p-value for days was found to be 0.684, for donor groups it was found to be 0.142 while for their interaction it was found to be 0.557 which were all greater than the significance level of 0.05 considered for the analysis.

3.1.3 Myogenin count

MyoG counts were calculated using the DAPI channel as a mask and using the Nucleus Counter on the overlayed image. MyoG was used to track the maturation state of myoblast in the muscle bundles through the time course as myogenin is expressed during the final differentiation stage when the fibers start fusing with one another. Figure 16 represents the MyoG counts obtained for each donor. For comparison between the donors the counts were normalized with the Cross-Sectional area of the respective bundles.

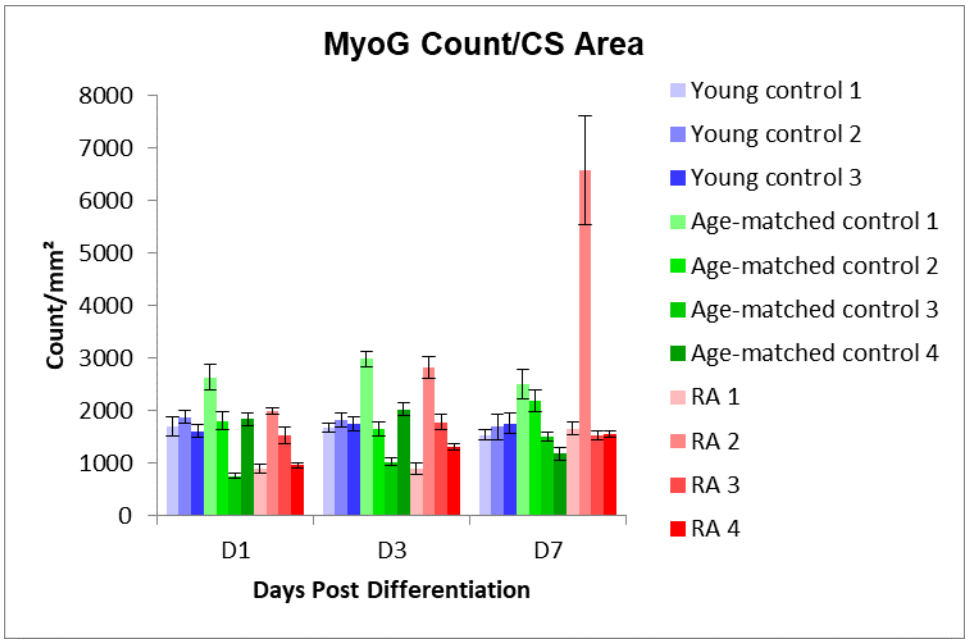

Figure 16: MyoG Count/CSA of myobundles for time course studies

For better comparison, all the donors in one group were averaged together and the results are summarized in figure 17. The myogenin count remained almost same with time for the controls though it increased with time for RA donors indicating the myofibers shifted towards fusion and maturation.

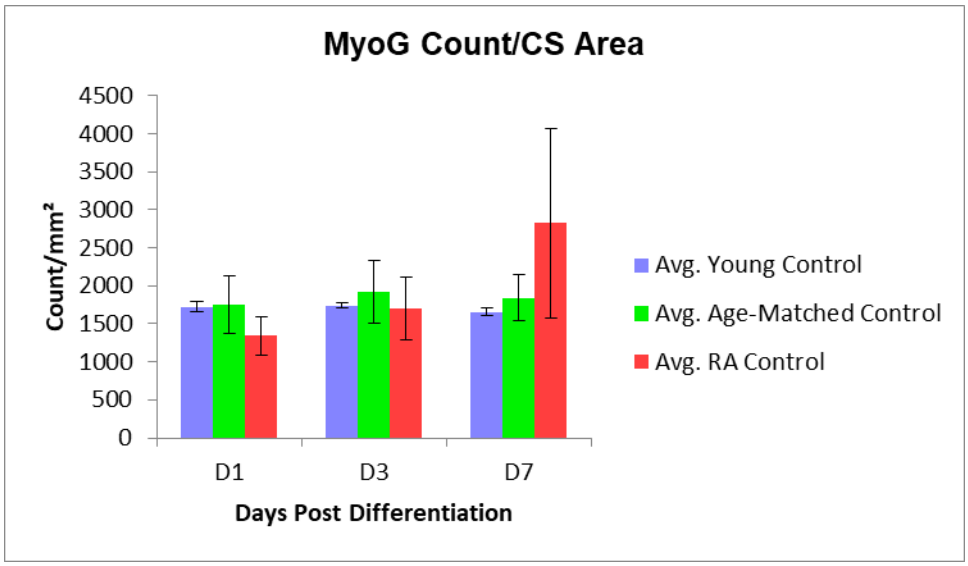

Figure 17: Averaged MyoG Count/CSA for time course studies

The two-way ANOVA results indicated that there were no statistically significant interactions between the donor groups and days-post differentiation on the nuclei count. The p-value for days was found to be 0.542, for donor groups it was found to be 0.868 while for their interaction it was found to be 0.595 which were all greater than the significance level of 0.05 considered for the analysis.

3.1.4 MyoG Count/Nuclei Count

The ratio was calculated to measure the proportion of mature cells in the myobundle. Figure 18 represents the data obtained for each donor.

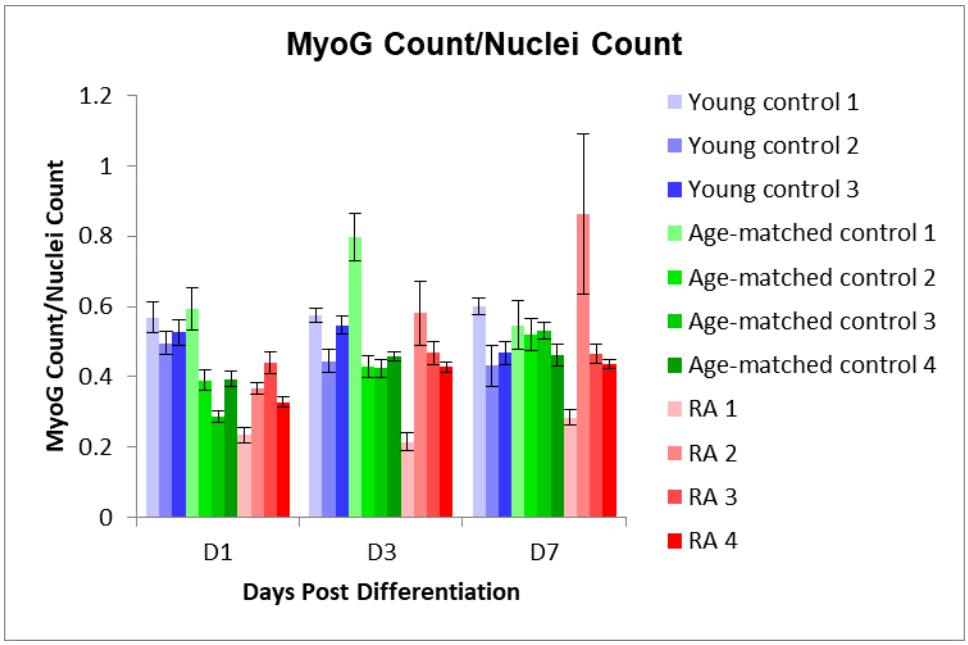

Figure 18: MyoG Count/Nuclei Count for time course studies

For better comparison, all the donors in one group were averaged together and the results are summarized in figure 19. The percentage of mature cells remained the same in young donors, while it increased with time in both age-matched controls and RA patients. This indicates that the myofibers were shifting toward fusion.

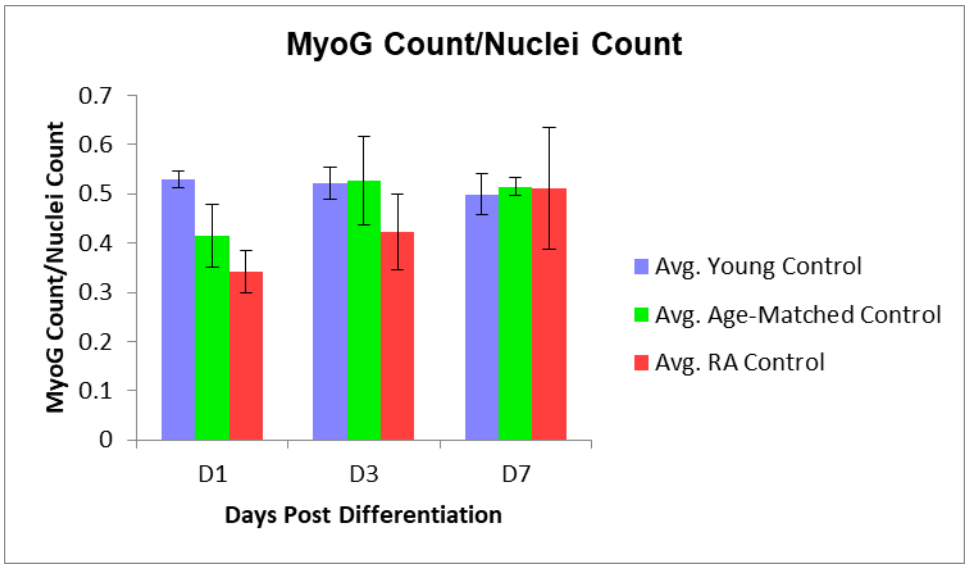

Figure 19: Averaged MyoG Count/Nuclei Count for time course studies

The two-way ANOVA results indicated that there were no statistically significant interactions between the donor groups and days-post differentiation on the nuclei count. The p-value for days was found to be 0.387, for donor groups it was found to be 0.313 while for their interaction it was found to be 0.708 which were all greater than the significance level of 0.05 considered for the analysis.

3.1.5 SAA+ Area/ Cross Sectional Area

Sarcomeric alpha actinin is responsible for anchoring actin filaments to the Z-line in the sarcomere and is responsible for stabilizing them against contractile forces. SAA positive area was calculated to measure the proportion of mature myotubes in the myobundle. For comparison between the donors the counts were normalized with the Cross-Sectional area of the respective bundles. Figure 20 represents the data obtained for each donor.

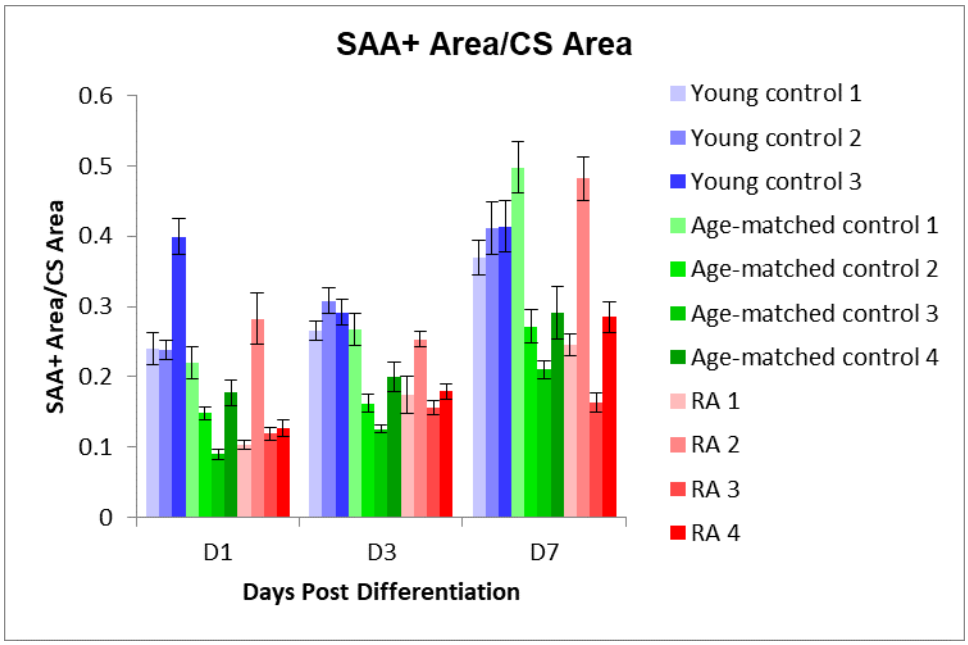

Figure 20 : SAA+ Area/CSA for time course studies

For better comparison, all the donors in one group were averaged together and the results are summarized in the figure 21. The SAA+ area increased with time in all three donor groups. The trend remained almost similar between the age-matched controls and RA donors, with higher SAA+ area in young controls which was expected since the regenerative capacity in young donors would be higher than the older donors, while it should be same between the age-matched controls and the RA patients.

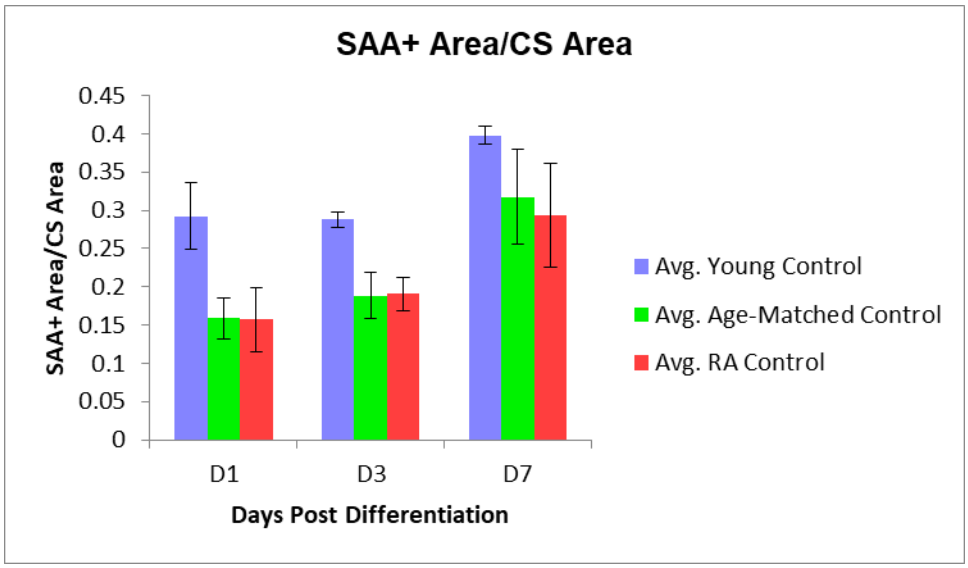

Figure 21: Averaged SAA+ Area/CSA for time course studies

The two-way ANOVA results indicated that there were no statistically significant interactions between the donor groups and days-post differentiation on the nuclei count (p=0.978 for interaction), though there were statistically significant differences between donor groups (p = 0.011) and time (p=0.002). Tukey test were performed to see which donor group had a significant variance for SAA+ Area. The test summary is showed in tables 3 and 4 below. The results indicated that there was a significant difference in SAA+ area between days 1 and 7 (p = 0.002) as well as days 3 and 7 (p=0.010). Also, there were significant differences between young controls and age-matched controls (p=0.024) as well as young controls and RA donors (p=0.015).

Table 3: Tukey Test results between donors for SAA+ Area

Multiple Comparisons

Dependent Variable: SAA+ Area/CS Area

Tukey HSD

(I) Donor Group	(J) Donor Group	Mean Difference (I-J)	Std. Error	Sig.	95% Confidence Interval	
					Lower Bound	Upper Bound
AM	RA	0.00769	0.034091	0.972	-0.07744	0.09283
	YG	-0.10452*	0.036823	0.024	-0.19648	-0.01256
RA	AM	-0.00769	0.034091	0.972	-0.09283	0.07744
	YG	-0.11221*	0.036823	0.015	-0.20417	-0.02026
YG	AM	0.10452*	0.036823	0.024	0.01256	0.19648
	RA	0.11221*	0.036823	0.015	0.02026	0.20417

Based on observed means.

The error term is Mean Square (Error) = 0.007.

*. The mean difference is significant at the 0.05 level.

Table 4: Tukey Test results between days for SAA+ Area

Multiple Comparisons

Dependent Variable: SAA+ Area/CS Area

Tukey HSD

(I) Day	(J) Day	Mean Difference (I-J)	Std. Error	Sig.	95% Confidence Interval	
					Lower Bound	Upper Bound
Day 1	Day 3	-0.02182	0.035607	0.815	-0.11074	0.06711
	Day 7	-0.13613*	0.035607	0.002	-0.22505	-0.04721
Day 3	Day 1	0.02182	0.035607	0.815	-0.06711	0.11074
	Day 7	-0.11431*	0.035607	0.010	-0.20323	-0.02539
Day 7	Day 1	0.13613*	0.035607	0.002	0.04721	0.22505
	Day 3	0.11431*	0.035607	0.010	0.02539	0.20323

Based on observed means.

The error term is Mean Square (Error) = 0.007.

*. The mean difference is significant at the 0.05 level.

3.1.6 Myofiber Diameter

Myofiber diameter were analyzed to monitor fusion of myofibers. Higher the fusion, the expected myofiber diameter should also be higher. Figure 22 represents the data obtained for each donor.

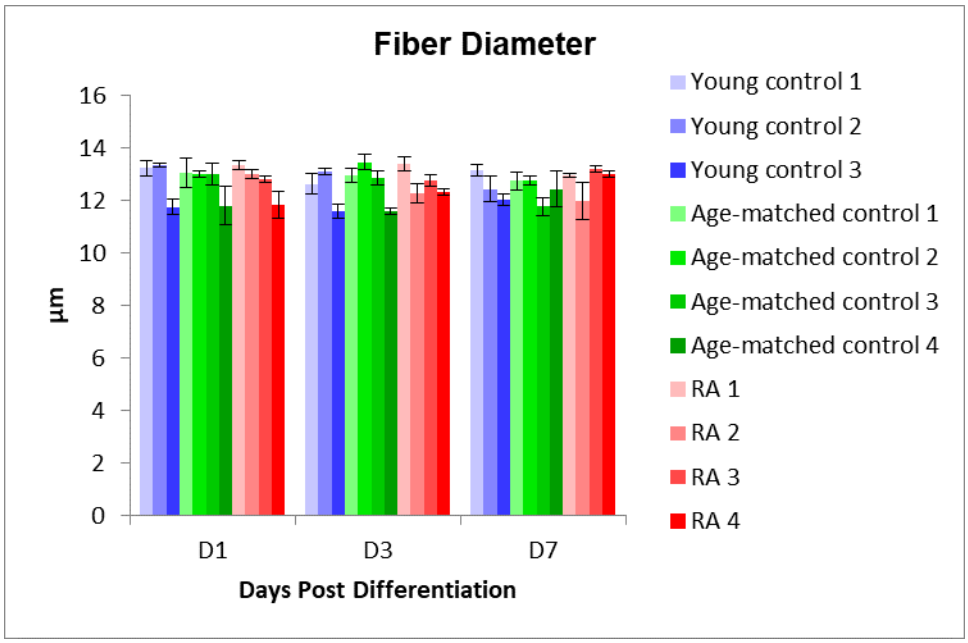

Figure 22: Myofiber Diameter for time course studies

For better comparison, all the donors in one group were averaged together and the results are summarized figure 23. The fiber diameter remained almost constant with time for all donors indicating that the myofibers did not fuse on a large magnitude even though they shifted towards maturation as indicated by the MyoG count and SAA+ area. The fiber diameters were found to be between 12 to 13µm which is comparable to normal average diameter of 10 µm for healthy donors.

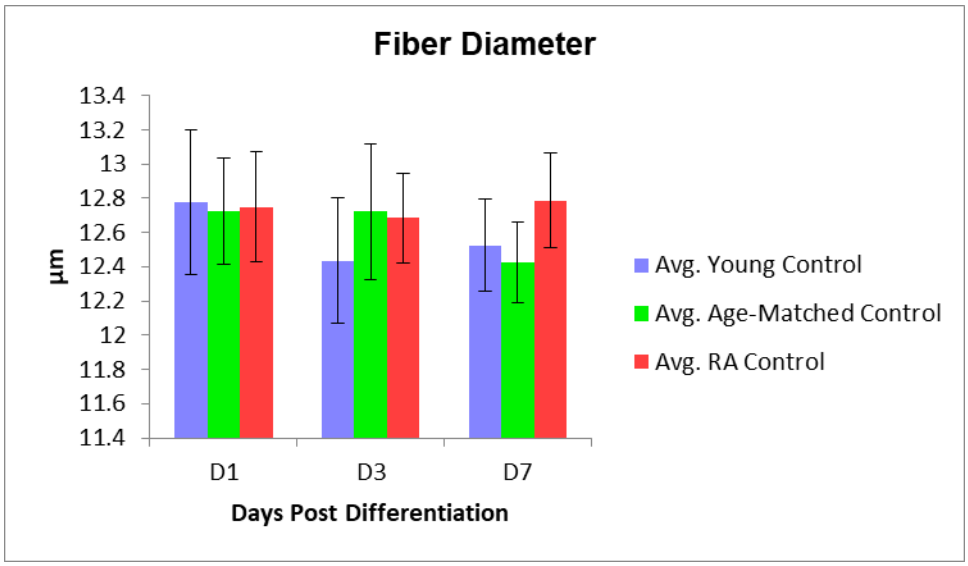

Figure 23: Averaged Myofiber Diameter for time course studies

The two-way ANOVA results indicated that there were no statistically significant interactions between the donor groups and days-post differentiation on the fiber diameter. The p-value for days was found to be 0.810, for donor groups it was found to be 0.839 while for their interaction it was found to be 0.951 which were all greater than the significance level of 0.05 considered for the analysis.

3.2 Cytokine Treatment studies

As with the time course studies, the cross-sections of myobundles taken at 10 days post-differentiation were analyzed using ImageJ for total cross-sectional area, nuclei count, MyoG count, SAA positive area and total fiber diameter. Table 5 summarizes the donors considered for cytokine treatments.

Table 5 : Donors characterized for cytokine treatments

Age-matched donors	RA donors
RAMC101 (2 bundles, 5 sections each)	RAE109 (2 bundles, 5 sections each)
RAMC105 (3 bundles, 5 sections each)	RAME100 (3 bundles, 5 sections each)
	RAME106 (2 bundles, 5 sections each)

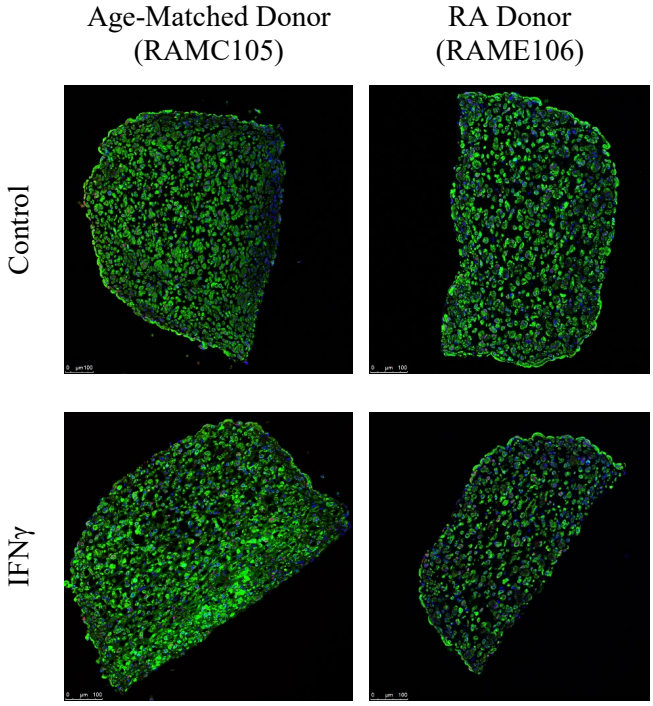

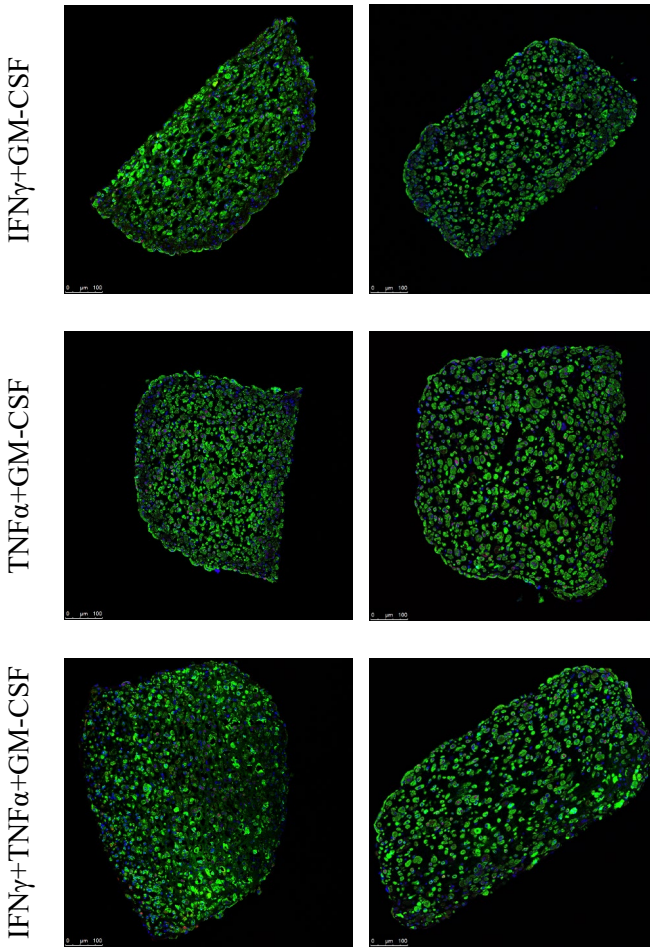

Figure 24: Cross-sections for each cytokine treatment

3.2.1 Cross-sectional area

The cross-sectional area was calculated in microns from ImageJ. Figure 25 represents the average cross-sectional area calculated for each donor at day 10 post differentiation for each of the cytokine treatment.

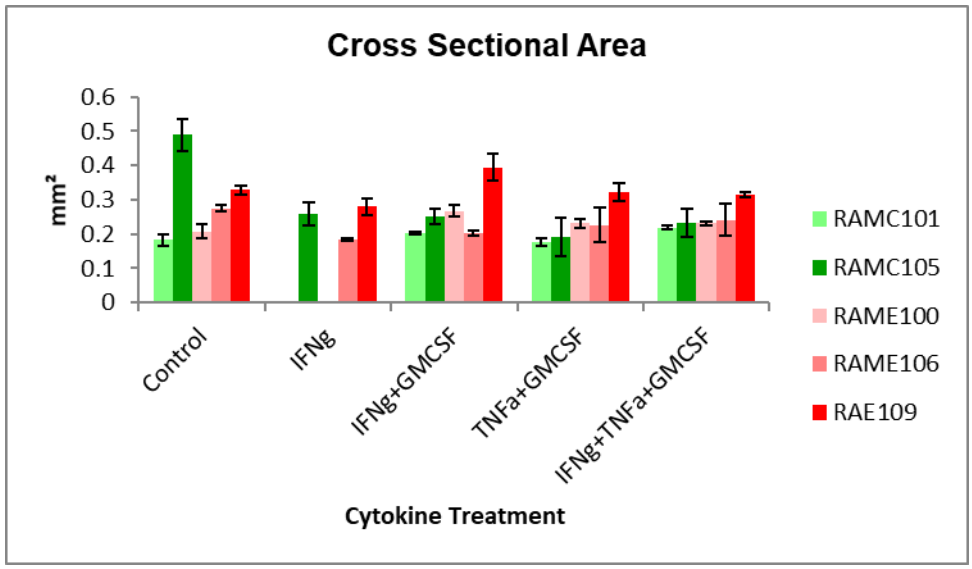

Figure 25 : Cross Sectional Area of myobundle for cytokine treatments

For better comparison, all the donors in one group were averaged together and the results are summarized in figure 26. The CSA decreased for aged-matched controls with treatments, while the CSA remained almost same with treatments for the RA donors.

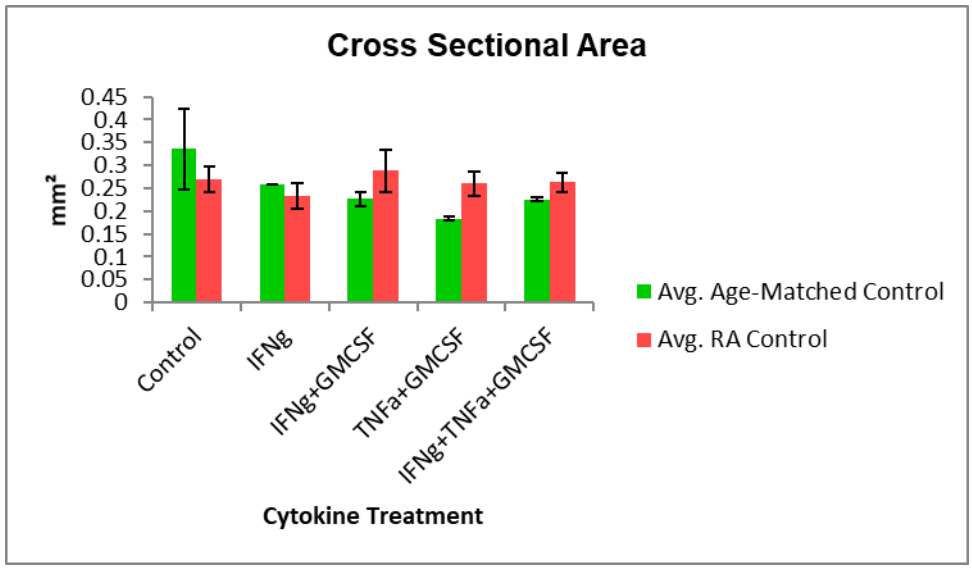

Figure 26: Average CSA for cytokine treatments

The two-way ANOVA results indicated that there were no statistically significant interactions between the donor groups and cytokine treatments on the CSA. The p-value for donor groups was found to be 0.661, for treatments it was found to be 0.654 while for their interaction it was found to be 0.671 which were all greater than the significance level of 0.05 considered for the analysis.

3.2.2 Nuclei Count

The Nuclei counts were calculated using the Nucleus Counter of the Particle Analysis Plugin of ImageJ. Nuclei counts were measured to access the number of cells in bundle and see the effect of maturation on the same. For comparison between the donors the counts were normalized with the Cross-Sectional area of the respective bundles. Figure 27 represents the Nuclei counts obtained for each donor.

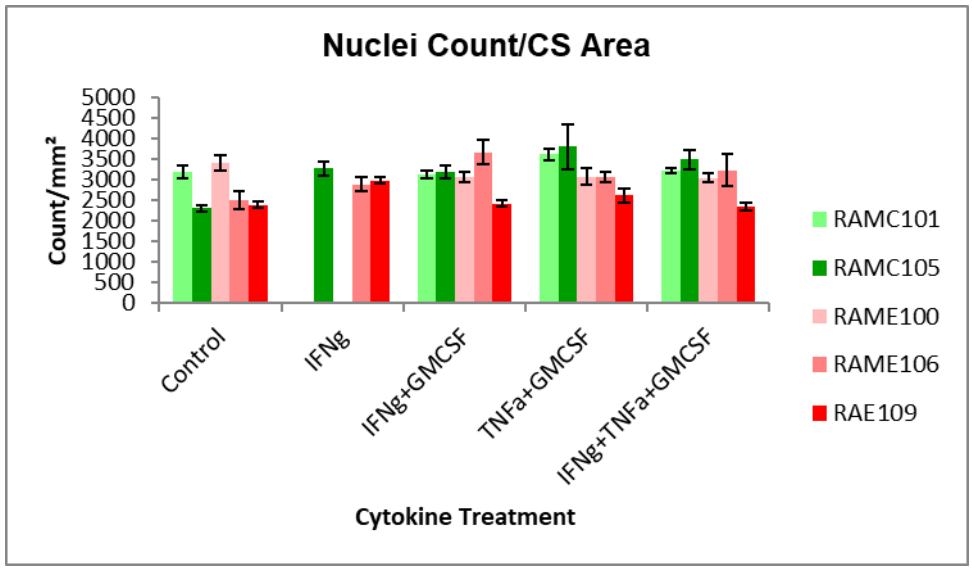

Figure 27: Nuclei Count/CSA of myobundles for cytokine treatments

For better comparison, all the donors in one group were averaged together and the results are summarized in figure 28. The nuclei count/cross sectional area of the myobundles from age-matched donors increased with treatments, while they remained almost the same for RA donors

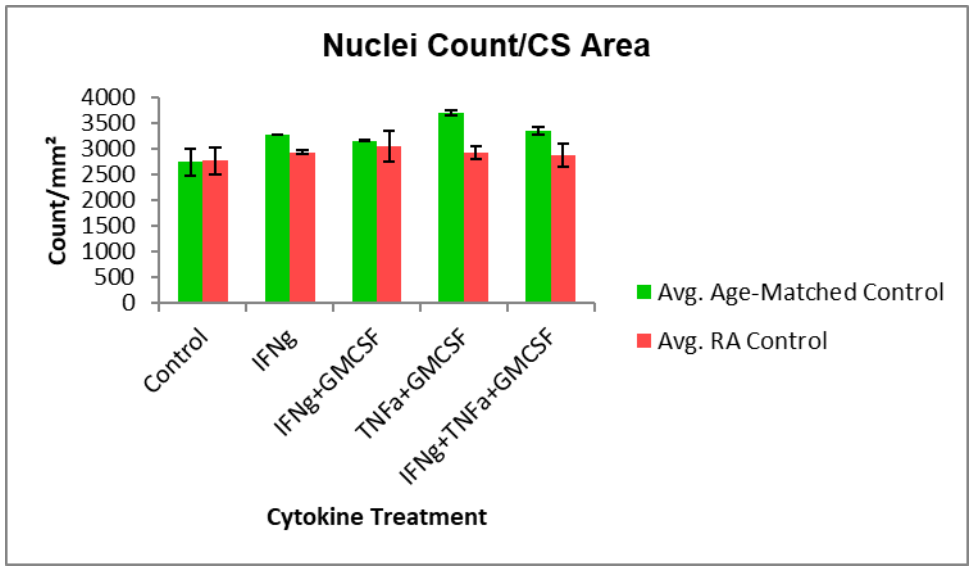

Figure 28: Averaged Nuclei Count for cytokine treatments

The two-way ANOVA results indicated that there were no statistically significant interactions between the donor groups and cytokine treatments on nuclei count. The p-value for donor groups was found to be 0.1, for treatments it was found to be 0.416 while for their interaction it was found to be 0.639 which were all greater than the significance level of 0.05 considered for the analysis.

3.2.3 Myogenin Count

MyoG counts were calculated using the DAPI channel as a mask and using the Nucleus Counter on the overlayed image. MyoG was used to track the maturation state of myoblast in the muscle bundles through the time course as myogenin is expressed during the final differentiation

stage when the fibers start fusing with one another. Figure 29 represents the MyoG counts obtained for each donor. For comparison between the donors the counts were normalized with the Cross-Sectional area of the respective bundles.

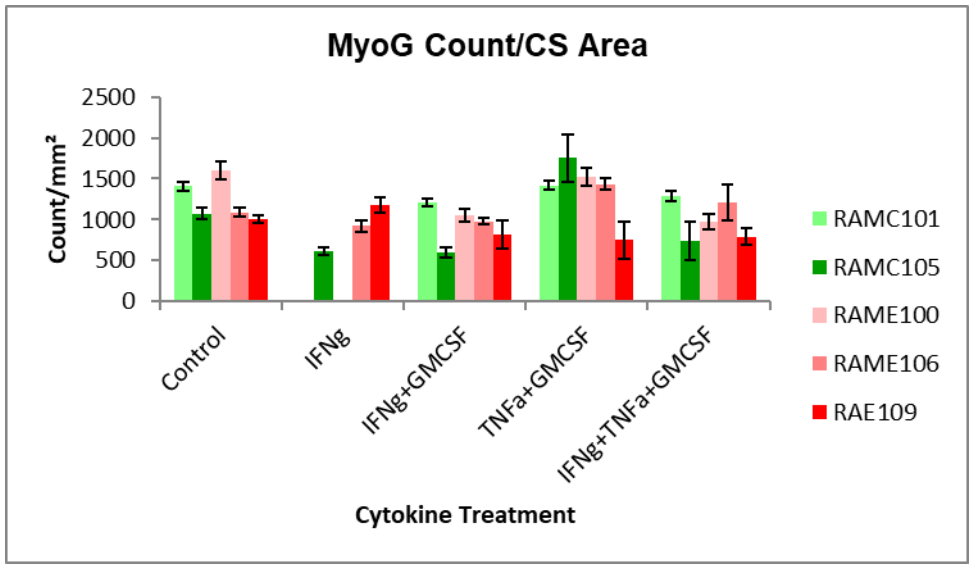

Figure 29: MyoG Count for cytokine treatments

For better comparison, all the donors in one group were averaged together and the results are summarized in figure 30. The myogenin count decreased on treatment with IFNγ, IFNγ+GMCSF, and IFNγ+TNFα+GMCSF but increased with treatment with TNFα+GMCSF for age-matched controls. For RA donors the count followed the same trend for treatments with IFNγ, IFNγ+GMCSF, and IFNγ+TNFα+GMCSF but remained almost the same for treatment with TNFα+GMCSF.

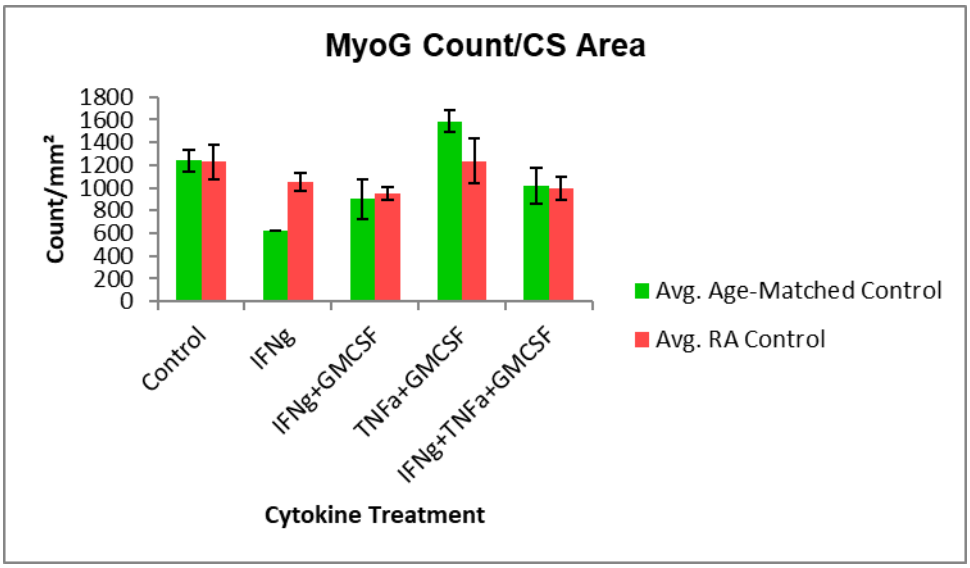

Figure 30: Averaged MyoG Count for cytokine treatments

The two-way ANOVA results indicated that there were no statistically significant interactions between the donor groups and cytokine treatments on the MyoG count. The p-value for donor groups was found to be 0.883, for treatments it was found to be 0.085 while for their interaction it was found to be 0.566 which were all greater than the significance level of 0.05 considered for the analysis.

3.2.4 MyoG Count/Nuclei Count

The ratio was calculated to measure the proportion of mature cells in the myobundle. Figure 31 represents the data obtained for each donor.

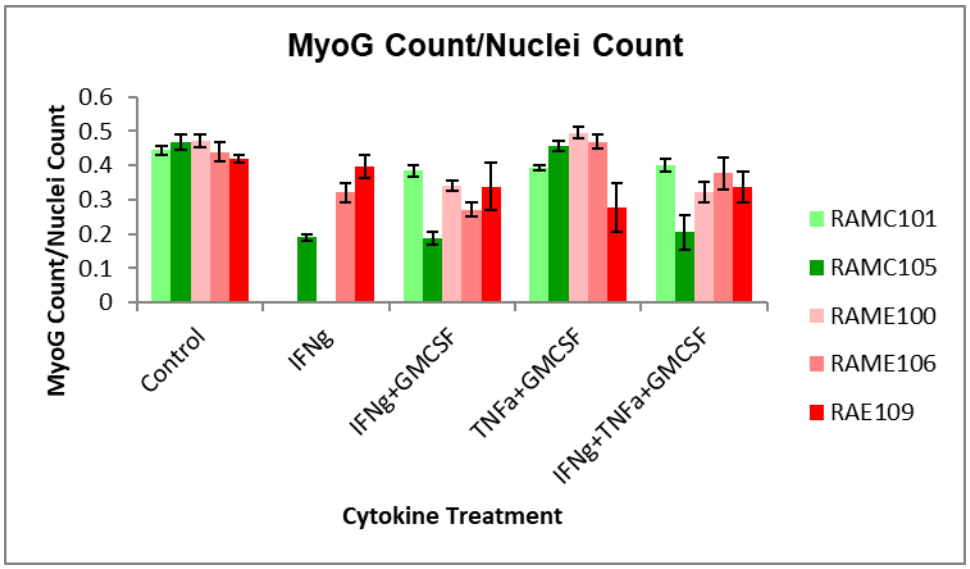

Figure 31: MyoG/Nuclei Count for cytokine treatments

For better comparison, all the donors in one group were averaged together and the results are summarized in figure 32. The percentage of mature cells remained almost the same on treatment with TNFα+GMCSF for both the age-matched donors and RA patients, while it decreased for both the donor groups on treatment with IFNγ, IFNγ+GMCSF and IFNγ+TNFα+GMCSF.

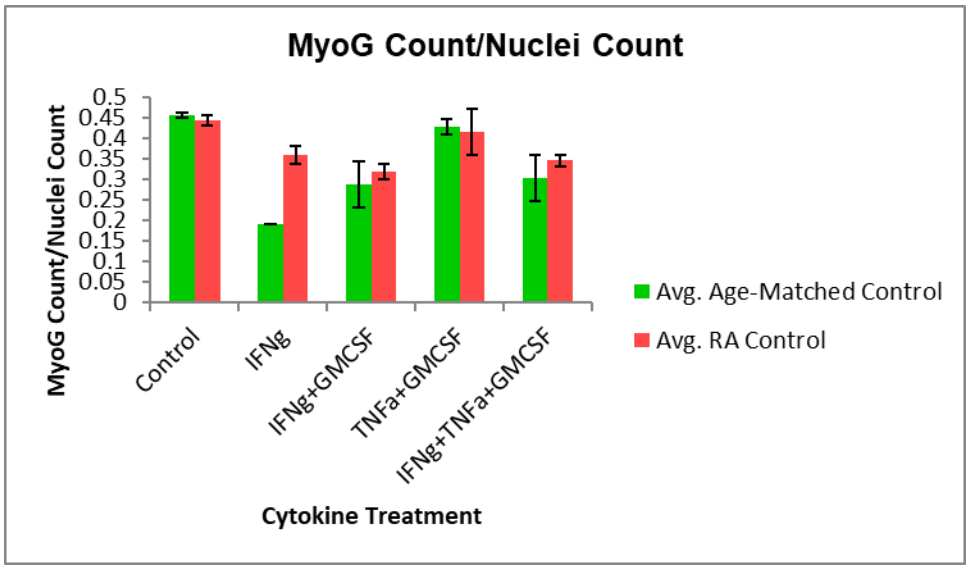

Figure 32: Averaged MyoG/Nuclei Count for cytokine treatments

The two-way ANOVA results indicated that there were no statistically significant interactions between the donor groups and cytokine treatments on the MyoG/Nuclei Count (p = 0.589 for interaction). Also, there was no statistically significant difference between the donor groups (p=0.222), but there were statistically significant differences between cytokine treatments (p = 0.023). Tukey test was performed to see which treatment showed a significant variance for MyoG/Nuclei Count, though the results indicated that there was no significant variance with any treatment. The test summary is showed in table 6 below.

Table 6: Tukey test results for treatments for MyoG count

Multiple Comparisons

Dependent Variable: MyoG/Nuclei Count

Tukey HSD

(I) Cytokine	(J) Cytokine	Mean Difference (I-J)	Std. Error	Sig.	95% Confidence Interval	
					Lower Bound	Upper Bound
Control	IFNg	0.14608	0.056503	0.131	-0.03183	0.32399
	IFNg+GMCSF	0.14379	0.048933	0.072	-0.01029	0.29787
	IFNg+TNFa+GMCSF	0.12032	0.048933	0.161	-0.03376	0.27439
	TNFa+GMCSF	0.03018	0.048933	0.970	-0.12389	0.18426
IFNg	Control	-0.14608	0.056503	0.131	-0.32399	0.03183
	IFNg+GMCSF	-0.00229	0.056503	1.000	-0.18020	0.17562
	IFNg+TNFa+GMCSF	0-.02576	0.056503	0.990	-0.20368	0.15215
	TNFa+GMCSF	-0.11590	0.056503	0.297	-0.29381	0.06201
IFNg+GMCSF	Control	-0.14379	0.048933	0.072	-0.29787	0.01029
	IFNg	0.00229	0.056503	1.000	-0.17562	0.18020
	IFNg+TNFa+GMCSF	-0.02347	0.048933	0.988	-0.17755	0.13060
	TNFa+GMCSF	-0.11361	0.048933	0.199	-0.26768	0.04047
IFNg+TNFa+GMCSF	Control	-0.12032	0.048933	0.161	-0.27439	0.03376
	IFNg	0.02576	0.056503	0.990	-0.15215	0.20368
	IFNg+GMCSF	0.02347	0.048933	0.988	-0.13060	0.17755
	TNFa+GMCSF	-0.09013	0.048933	0.392	-0.24421	0.06394
TNFa+GMCSF	Control	-0.03018	0.048933	0.970	-0.18426	0.12389
	IFNg	0.11590	0.056503	0.297	-0.06201	0.29381
	IFNg+GMCSF	0.11361	0.048933	0.199	-0.04047	0.26768
	IFNg+TNFa+GMCSF	0.09013	0.048933	0.392	-0.06394	0.24421

Based on observed means.
The error term is Mean Square (Error) = 0.006.

3.2.5 SAA+ Area/ Cross Sectional Area

Sarcomeric alpha actinin is responsible for anchoring actin filaments to the Z-line in the sarcomere and is responsible for stabilizing them against contractile forces. SAA positive area was calculated to measure the proportion of mature myotubes in the myobundle. For comparison between the donors the counts were normalized with the Cross-Sectional area of the respective bundles. Figure 33 represents the data obtained for each donor.

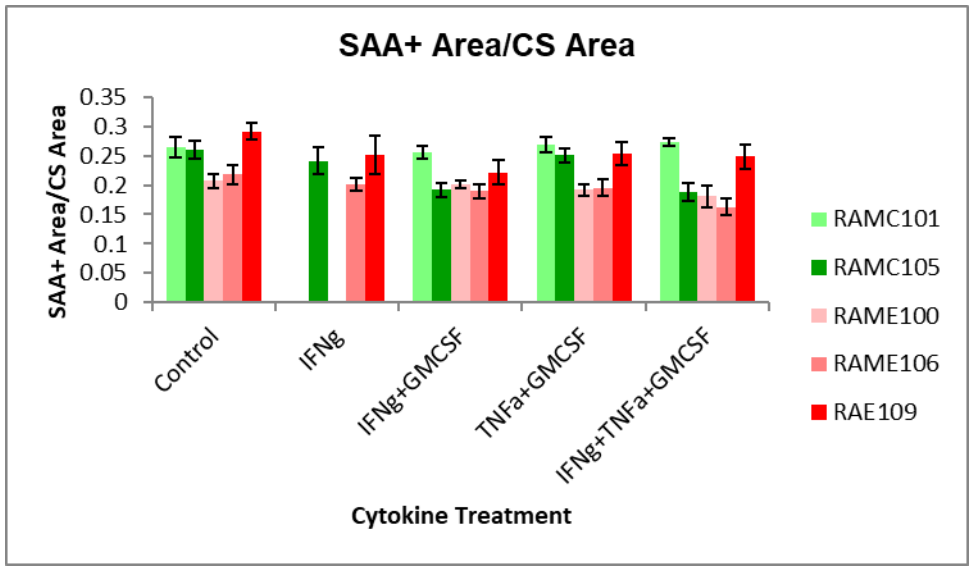

Figure 33: SAA+ Area for cytokine treatments

For better comparison, all the donors in one group were averaged together and the results are summarized in figure 34. The SAA+ area decreased with all treatments for both the donor groups.

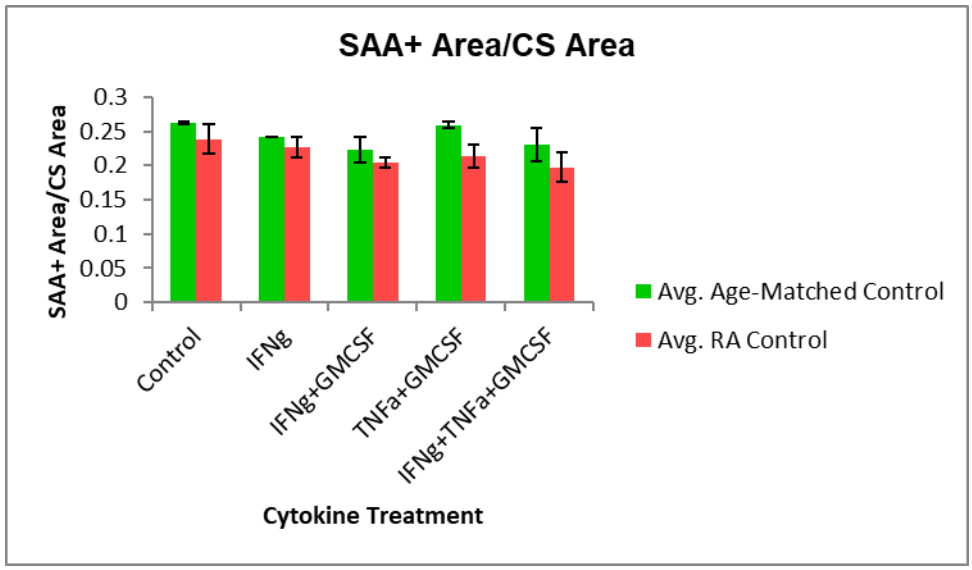

Figure 34: Averaged SAA+ Area for cytokine treatments

The two-way ANOVA results indicated that there were no statistically significant interactions between the donor groups and cytokine treatments on the SAA area. The p-value for donor groups was found to be 0.122, for treatments it was found to be 0.520 while for their interaction it was found to be 0.977 which were all greater than the significance level of 0.05 considered for the analysis.

3.2.6 Myofiber Diameter

Myofiber diameter were analyzed to monitor fusion of myofibers. Higher the fusion, the expected myofiber diameter should also be higher. Figure 35 represents the data obtained for each donor.

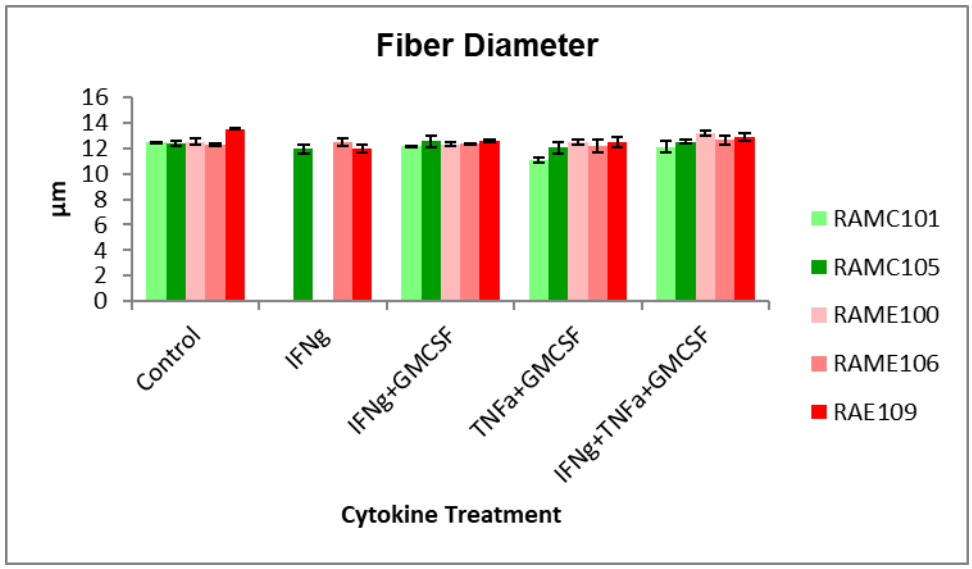

Figure 35: Myofiber Diameter for cytokine treatments

For better comparison, all the donors in one group were averaged together and the results are summarized in the figure 36. The fiber diameter decreased on treatment with IFNγ, TNFα+GMCSF but remained almost the same on treatment with IFNγ+GMCSF and IFNγ+TNFα+GMCSF for the age-matched controls. The fiber diameter decreased on treatment with IFNγ, TNFα+GMCSF and IFNγ+GMCSF but increased on treatment with IFNγ+TNFα+GMCSF for RA donors.

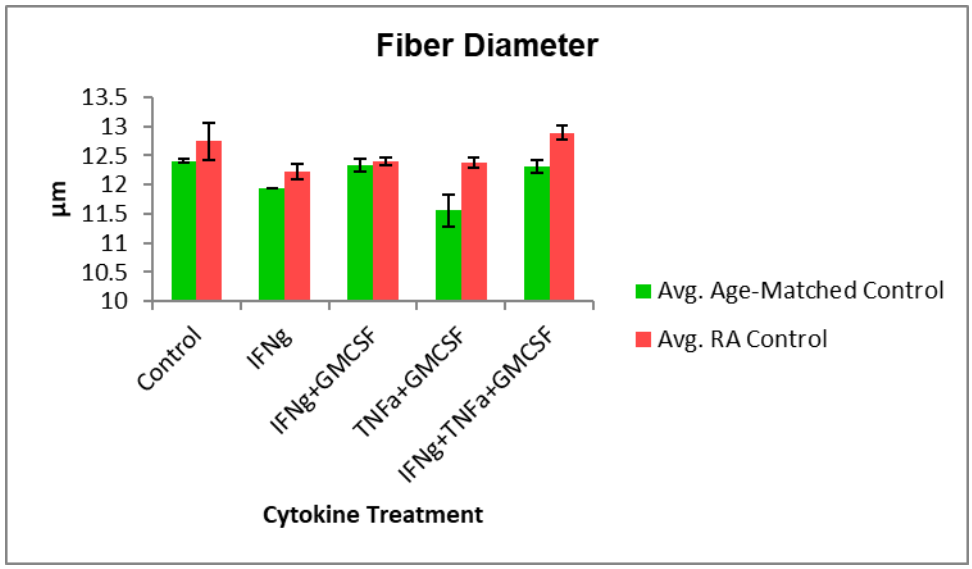

Figure 36: Averaged Fiber Diameter for cytokine treatments

The two-way ANOVA results indicated that there were no statistically significant interactions (p=0.610 for interaction). Also, there was no statistically significant difference in cytokine treatments (p = 0.092), but there were statistically significant differences between donor groups (p = 0.025). Hence RA influenced fiber diameter as compared to age-matched controls.

4. Conclusions

In the presented work, we characterized tissue engineered skeletal muscle bundles for disease specific traits of Rheumatoid Arthritis (RA) as the muscle bundle matures. For the characterization, young donors, age-matched donors and RA patients were considered by taking the human skeletal muscle samples from vastus lateralis muscle (hamstring muscle for young donors) through a biopsy for each donor. The obtained samples were purified for hSkM and expanded for preparation of myobundles. The cross-sections of the myobundles were analyzed for expression of myogenin, sarcomeric alpha actinin and the total nuclei count at days 1 ,3 and 7 post-differentiation to see variance in each parameter through the maturation. Moreover, we also were able to replicate the pro-inflammatory phenotype of RA in myobundles through cytokine treatments. The cytokine treated bundles were also characterized for the same traits as the time-course studies, but the bundles were characterized at day 10 post-differentiation.

For the time course studies, cross-sectional area of the engineered myobundles decreased slightly from D1 to D7 for RA donors as compared to the young donors as well as the age-matched controls. The area was found to be around 0.2-0.25mm. The Nuclei count for young controls remained same through the time-course but for age-matched controls the count decreased with time, while they increased for RA donors. For RA donors the nuclei count was found to be around 5000/mm^2 at day 7 post-differentiation. The MyoG counts for the young donors and age-matched controls were found to be almost the same and the counts increased for RA donors, which were found to be around 3000/mm^2 at 7 days post differentiation. The proportion of MyoG/Nuclei count remained the same for the young donors but increased slightly for age-matched controls and RA donors and was found to be around 50% at day 7 post-differentiation.

The SAA+ area increased throughout the time course for all donors, at D7 post-differentiation the SAA+ was found to be 30% for both the age-matched control and the RA donors, while it was found to be 40% for the young controls. The myofiber diameter remained almost constant with time for all donors indicating that the myofibers did not fuse on a large magnitude even though they shifted towards maturation as indicated by the MyoG count and SAA+ area. The fiber diameters were found to be between 12 to 13μm which is comparable to normal average diameter of 10 μm for healthy donors.

According to our hypothesis, the pro-inflammatory cytokines and macrophages should be acting on skeletal muscle causing reduction in regeneration ability and force reduction hence we should be observing a reduction in fiber formation. Though, according to our results, the cross-sectional area of the bundles remained almost the same throughout the time course, with an increase in nuclei count/CSA and MyoG count/CSA indicating that the myoblasts were shifting towards end stage differentiation and fusion. Also, almost 50% of the myoblasts expressed myogenin at day 7 post differentiation which further affirms that the cells were shifting towards maturation. Moreover, the SAA+ area also increased for RA donors and almost 30% of the CSA was found to be SAA+ indicating that the myotube had started forming since once the cells differentiate and fuse into myotubes they start expressing α-actinin and myosin heavy chain. Despite the increase in MyoG count and the SAA+ area the myofiber diameter remained almost the same and was found to be between 12 to 13 μm. These results indicate that, there was negligible reduction in fiber formation and force production. This may be because of medications taken by the RA patient which might be helping the muscle function. Another possible reason might be that the cells were taken out from the inflammatory environment and might no longer be affected by the pro-inflammatory cytokines and hence regained their normal functions.

We then moved forward to replicate the disease pro-inflammatory phenotype by carrying out cytokine treatments on the engineered myobundles. IFNγ, IFNγ+GMCSF, TNFα+GMCSF and IFNγ+TNFα+GMCSF were chosen for the cytokine treatments. The cross-sectional area decreased for the aged-matched control for all cytokine treatments as compared to the control, while remained almost the same for treatment all treatments for RA bundles. The Nuclei count/ CSA increased for all the treatments for the age-matched controls, while they remained almost the same for the RA bundles. The MyoG count/CSA decreased for all treatments except TNFα+GMCSF for which it increased for age-matched controls, while for the RA donors it remained almost the same. The percentage of cell expressing myogenin decreased for both the age-matched control and the RA donors for all the cytokine treatments except TNFα+GMCSF for which it remained the same. The SAA+ area decreased for all the conditions for both the RA donors and age-matched controls. Lastly, the fiber diameter decreased on treatment with IFNγ, TNFα+GMCSF but remained almost the same on treatment with IFNγ+GMCSF and IFNγ+TNFα+GMCSF for the age-matched controls. The fiber diameter decreased on treatment with IFNγ, TNFα+GMCSF and IFNγ+GMCSF but increased on treatment with IFNγ+TNFα+GMCSF for RA donors. Hence, according to our results, the cross-sectional area, MyoG count/CSA, MyoG/Nuclei count, SAA+ area and the myofiber diameter each decreased with cytokine treatments indicating that the cytokines may indeed affect the skeletal muscle cells and as a result compromise their function and reduce the regeneration ability of skeletal muscle cells. Though when we performed Tukey test for the results found to be statistically significant through ANOVA, we could not find any positive correlation. This may be due to the small number of donors considered in the study, increasing which might give us more insight into the effect of cytokine treatments on the maturation of skeletal muscle bundles in RA.

We can say that cytokines play a role in disease development and progression through our cytokine treatment studies, though it is not conclusive from our time course studies, for which a longer time course for up to 10 days post-differentiation or more may be considered. Also, more patient data regarding the disease severity and medications taken by the patients might also be helpful.

Appendix A: Two-way ANOVA results generated through SPSS tool for time course studies

Tests of Between-Subjects Effects

Dependent Variable: CS Area (mm^2)

Source	Type III Sum of Squares	Df	Mean Square	F	Sig.
Corrected Model	0.013[a]	8	0.002	0.532	0.821
Intercept	1.608	1	1.608	528.059	0.000
Donor Group	0.007	2	0.004	1.178	0.325
Day	0.000	2	0.000	0.076	0.927
Donor Group * Day	0.005	4	0.001	0.425	0.789
Error	0.073	24	0.003		
Total	1.695	33			
Corrected Total	0.086	32			

a. R Squared = 0.151 (Adjusted R Squared = -0.133)

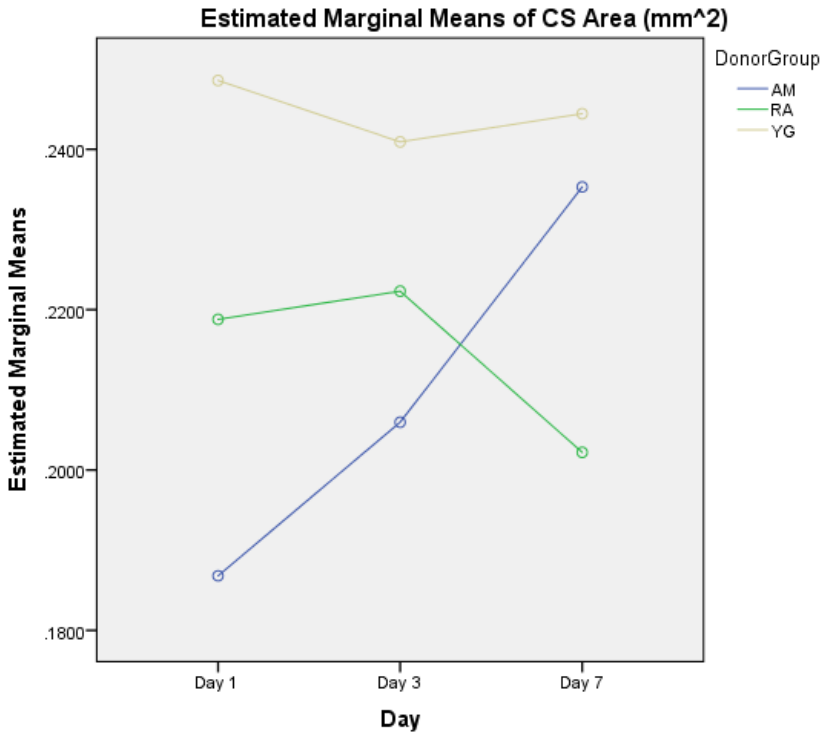

Tests of Between-Subjects Effects

Dependent Variable: Nuclei/CS Area (count/mm^2)

Source	Type III Sum of Squares	df	Mean Square	F	Sig.
Corrected Model	12037211.313[a]	8	1504651.414	1.028	0.442
Intercept	479133680.837	1	479133680.837	327.419	0.000
Donor Group	6200773.003	2	3100386.502	2.119	0.142
Day	1130204.978	2	565102.489	0.386	0.684
Donor Group * Day	4492048.253	4	1123012.063	0.767	0.557
Error	35120724.498	24	1463363.521		
Total	546554894.429	33			
Corrected Total	47157935.810	32			

a. R Squared = 0.255 (Adjusted R Squared = 0.007)

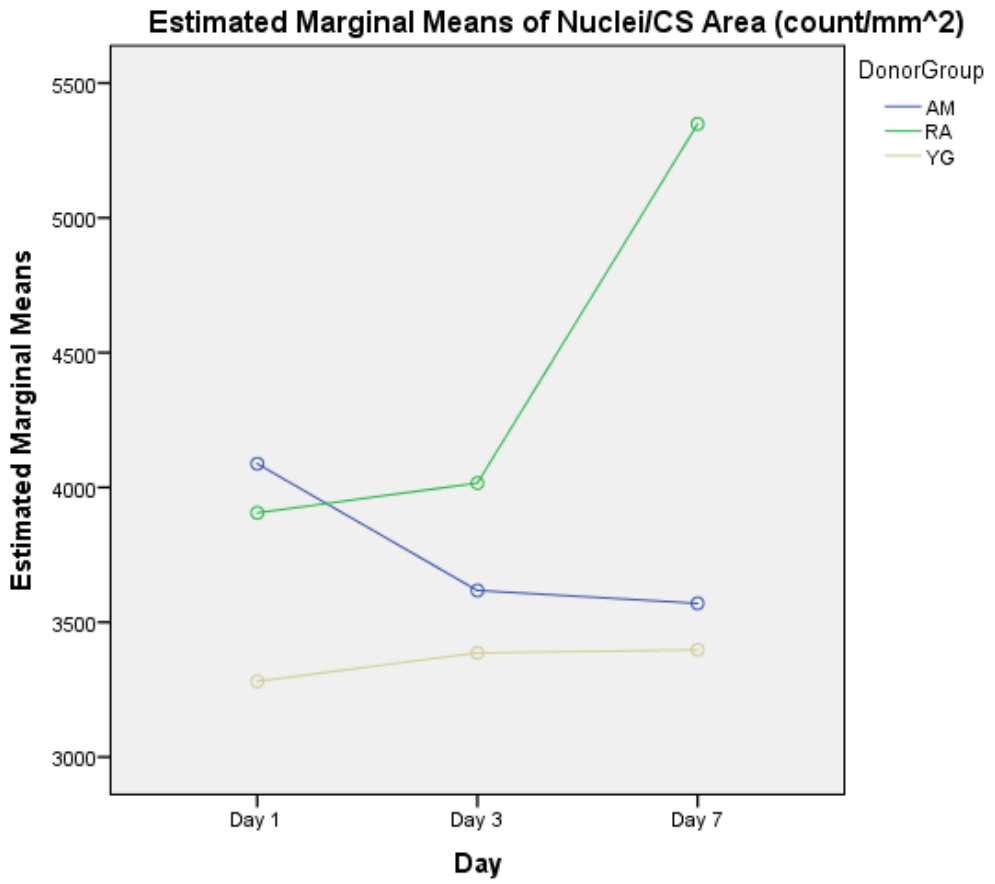

Tests of Between-Subjects Effects

Dependent Variable: MyoG/CS Area (count/mm^2)

Source	Type III Sum of Squares	df	Mean Square	F	Sig.
Corrected Model	5178351.350[a]	8	647293.919	0.584	0.781
Intercept	108624607.477	1	108624607.477	98.068	0.000
Donor Group	315717.823	2	157858.912	0.143	0.868
Day	1392361.808	2	696180.904	0.629	0.542
Donor Group * Day	3131721.113	4	782930.278	0.707	0.595
Error	26583542.018	24	1107647.584		
Total	143781451.013	33			
Corrected Total	31761893.368	32			

a. R Squared = 0.163 (Adjusted R Squared = -0.116)

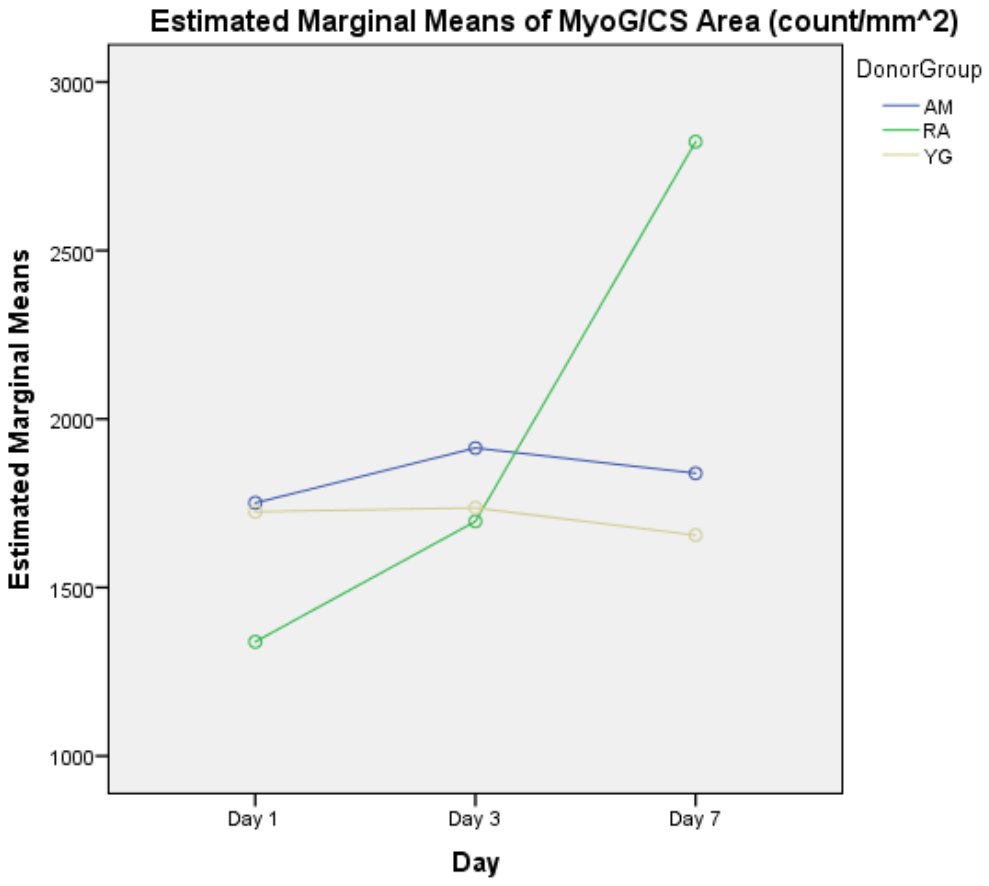

Tests of Between-Subjects Effects

Dependent Variable: MyoG Count/Nuclei Count

Source	Type III Sum of Squares	df	Mean Square	F	Sig.
Corrected Model	0.135[a]	8	0.017	0.890	0.540
Intercept	7.338	1	7.338	387.195	0.000
Donor Group	0.046	2	0.023	1.218	0.313
Day	0.037	2	0.019	0.989	0.387
Donor Group * Day	0.041	4	0.010	0.539	0.708
Error	0.455	24	0.019		
Total	7.948	33			
Corrected Total	0.590	32			

a. R Squared = 0.229 (Adjusted R Squared = -0.028)

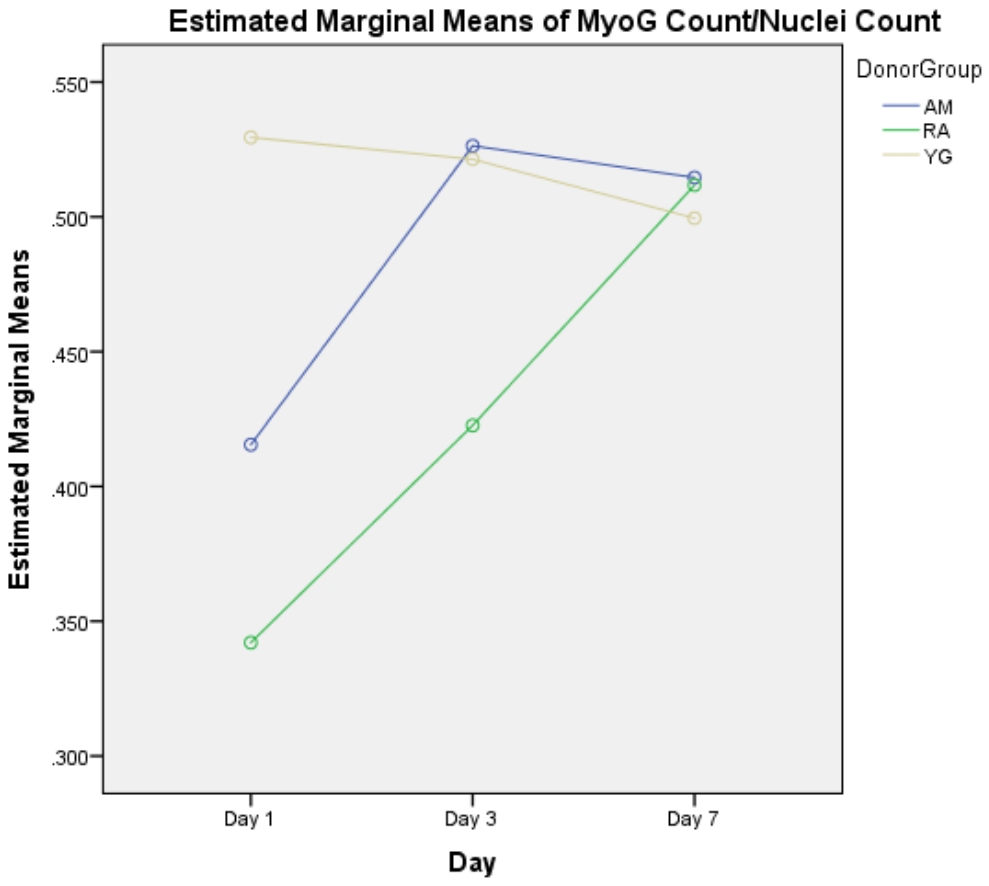

Tests of Between-Subjects Effects

Dependent Variable: SAA+ Area/CS Area

Source	Type III Sum of Squares	df	Mean Square	F	Sig.
Corrected Model	0.198[a]	8	0.025	3.547	0.008
Intercept	2.089	1	2.089	299.556	0.000
Donor Group	0.077	2	0.039	5.537	0.011
Day	0.112	2	0.056	8.058	0.002
Donor Group * Day	0.003	4	0.001	0.109	0.978
Error	0.167	24	0.007		
Total	2.384	33			
Corrected Total	0.365	32			

a. R Squared = 0.542 (Adjusted R Squared = 0.389)

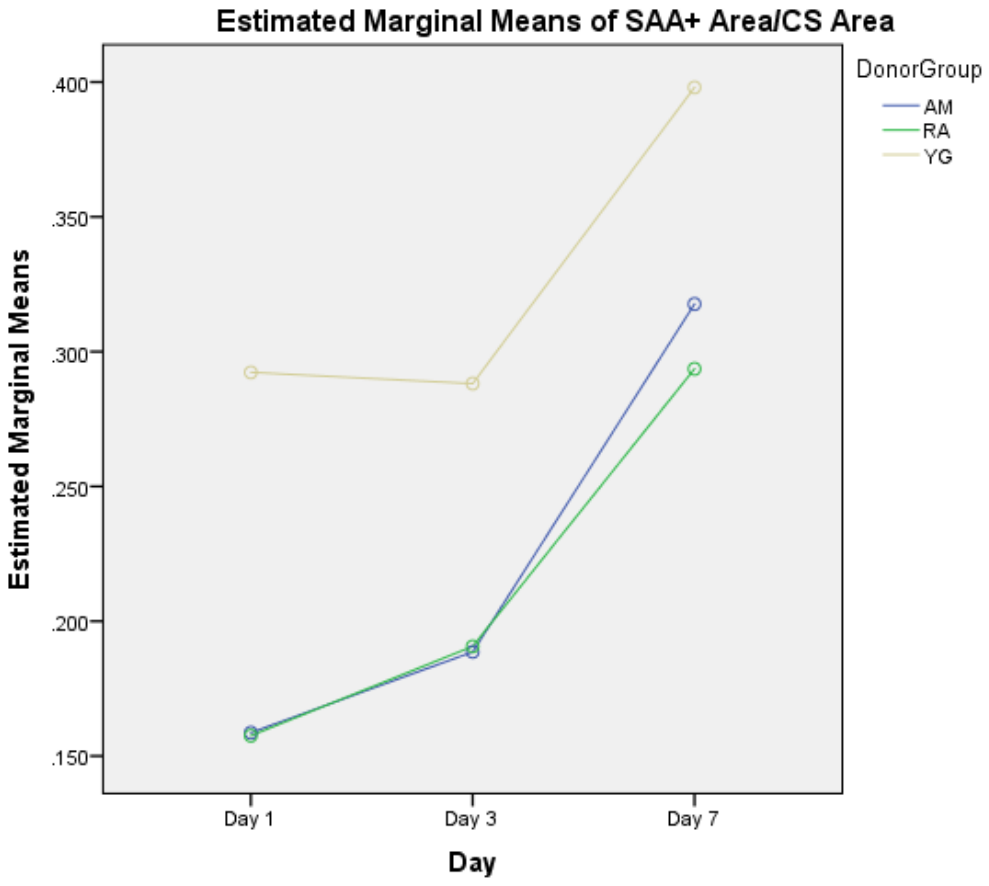

Tests of Between-Subjects Effects

Dependent Variable: Fiber Diameter (µm)

Source	Type III Sum of Squares	df	Mean Square	F	Sig.
Corrected Model	0.595[a]	8	0.074	0.177	0.992
Intercept	5182.529	1	5182.529	12310.005	0.000
Donor Group	0.149	2	0.075	0.177	0.839
Day	0.179	2	0.089	0.212	0.810
Donor Group * Day	0.287	4	0.072	0.171	0.951
Error	10.104	24	0.421		
Total	5294.394	33			
Corrected Total	10.699	32			

a. R Squared = 0.056 (Adjusted R Squared = -0.259)

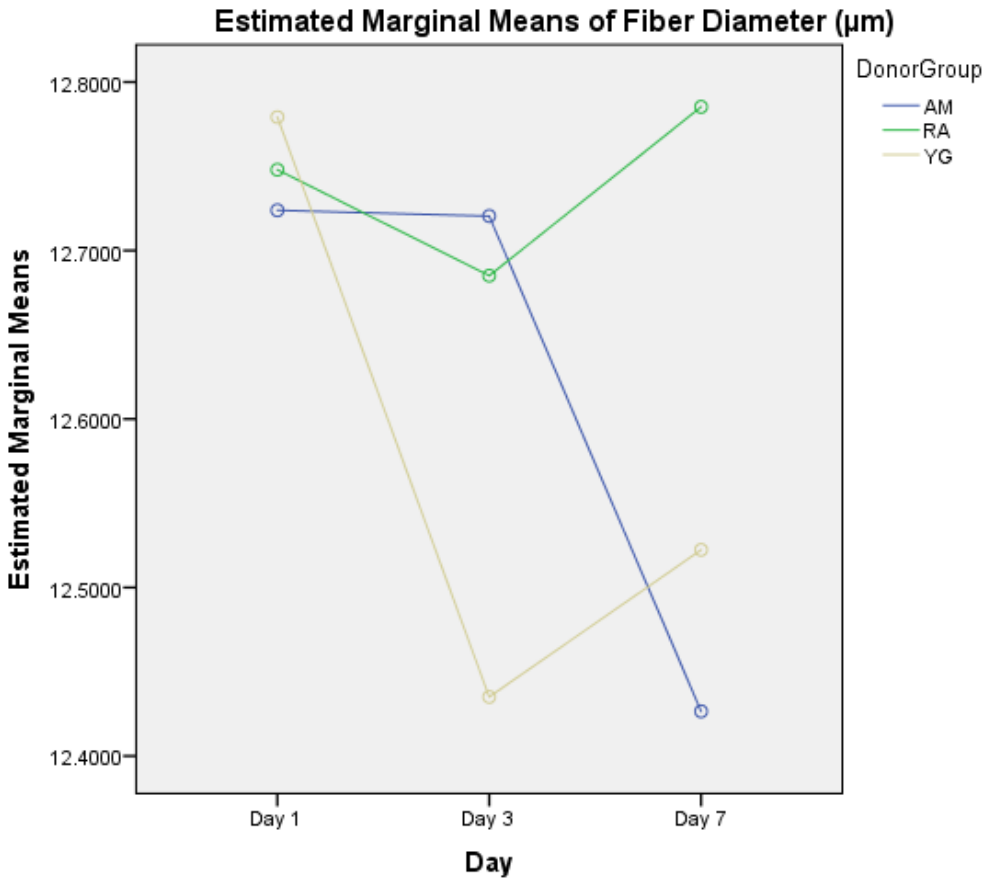

Appendix B: Two-way ANOVA results generated through SPSS tool for cytokine treatment studies

Tests of Between-Subjects Effects

Dependent Variable: CS Area (mm^2)

Source	Type III Sum of Squares	df	Mean Square	F	Sig.
Corrected Model	0.032[a]	9	0.004	0.512	0.841
Intercept	1.338	1	1.338	193.854	0.000
Donor Group	0.001	1	0.001	0.201	0.661
Cytokine	0.017	4	0.004	0.624	0.654
Donor Group * Cytokine	0.016	4	0.004	0.597	0.671
Error	0.090	13	0.007		
Total	1.638	23			
Corrected Total	0.122	22			

a. R Squared = 0.262 (Adjusted R Squared = -0.249)

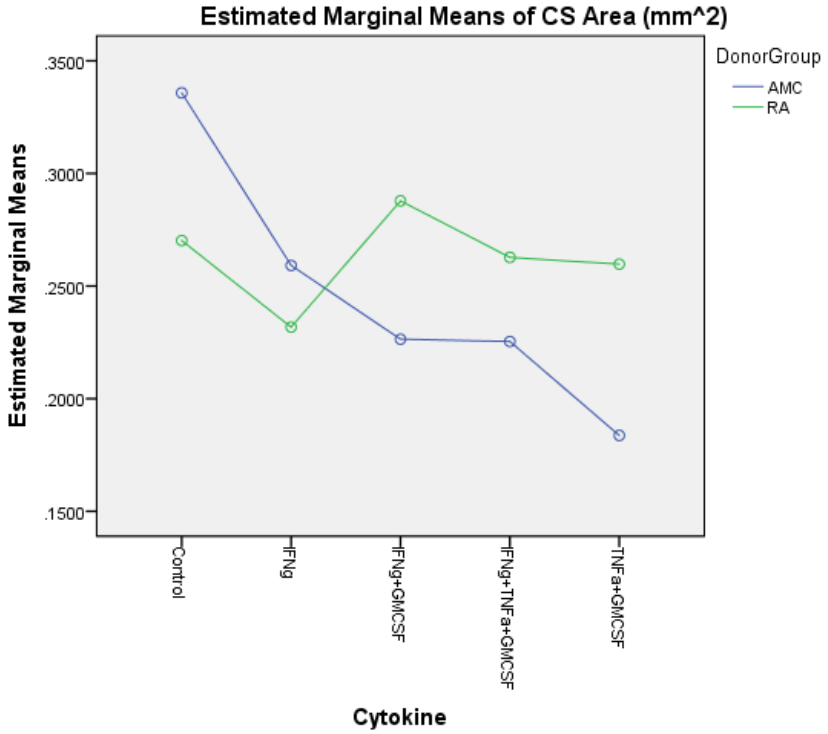

Tests of Between-Subjects Effects

Dependent Variable: Nuclei/CS Area (count/mm^2)

Source	Type III Sum of Squares	df	Mean Square	F	Sig.
Corrected Model	1713795.282[a]	9	190421.698	1.026	0.469
Intercept	195378748.072	1	195378748.072	1052.653	0.000
Donor Group	583751.691	1	583751.691	3.145	0.100
Cytokine	784993.535	4	196248.384	1.057	0.416
Donor Group * Cytokine	479815.438	4	119953.860	0.646	0.639
Error	2412878.894	13	185606.069		
Total	215894115.681	23			
Corrected Total	4126674.176	22			

a. R Squared = 0.415 (Adjusted R Squared = 0.011)

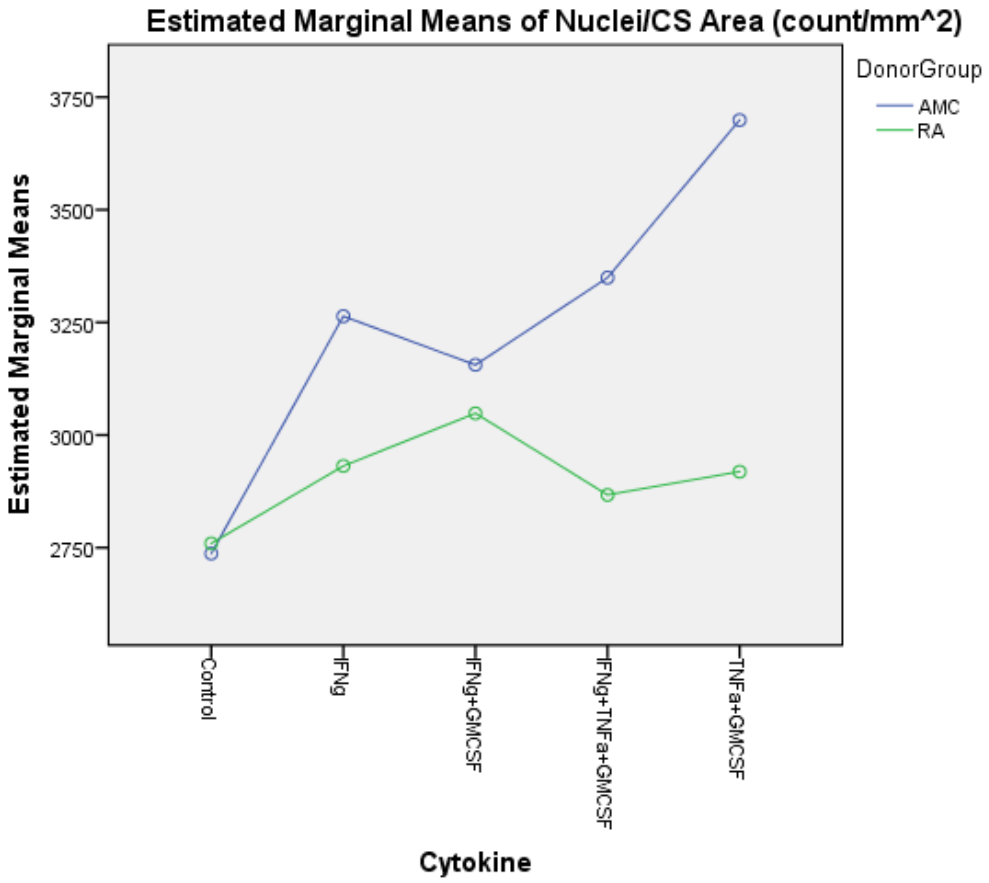

Tests of Between-Subjects Effects

Dependent Variable: MyoG/CS Area (count/mm^2)

Source	Type III Sum of Squares	df	Mean Square	F	Sig.
Corrected Model	1046729.838[a]	9	116303.315	1.307	0.320
Intercept	24248140.036	1	24248140.036	272.564	0.000
Donor Group	2005.158	1	2005.158	0.023	0.883
Cytokine	926096.025	4	231524.006	2.602	0.085
Donor Group * Cytokine	272759.921	4	68189.980	0.766	0.566
Error	1156520.536	13	88963.118		
Total	30345186.704	23			
Corrected Total	2203250.374	22			

a. R Squared = 0.475 (Adjusted R Squared = 0.112)

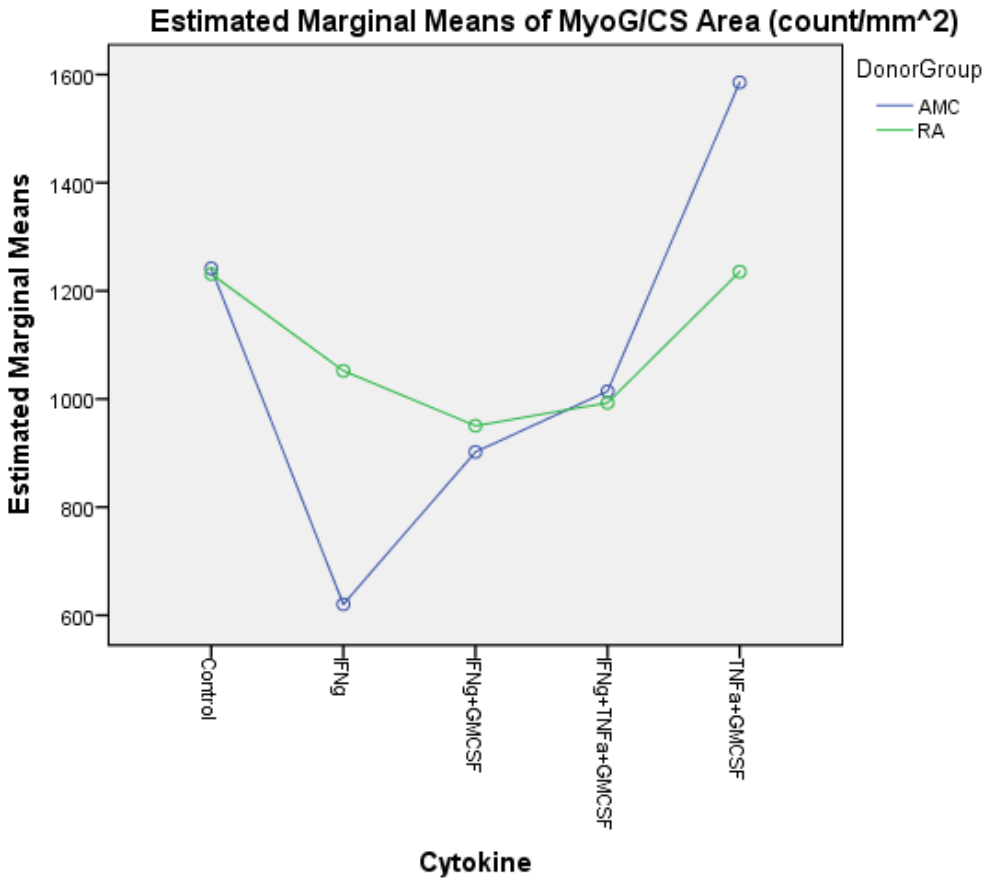

Tests of Between-Subjects Effects

Dependent Variable: MyoG/Nuclei Count

Source	Type III Sum of Squares	df	Mean Square	F	Sig.
Corrected Model	0.109[a]	9	0.012	2.015	0.122
Intercept	2.598	1	2.598	433.936	0.000
Donor Group	0.010	1	0.010	1.644	0.222
Cytokine	0.098	4	0.024	4.085	0.023
Donor Group * Cytokine	0.017	4	0.004	0.728	0.589
Error	0.078	13	0.006		
Total	3.267	23			
Corrected Total	0.186	22			

a. R Squared = 0.582 (Adjusted R Squared = 0.293)

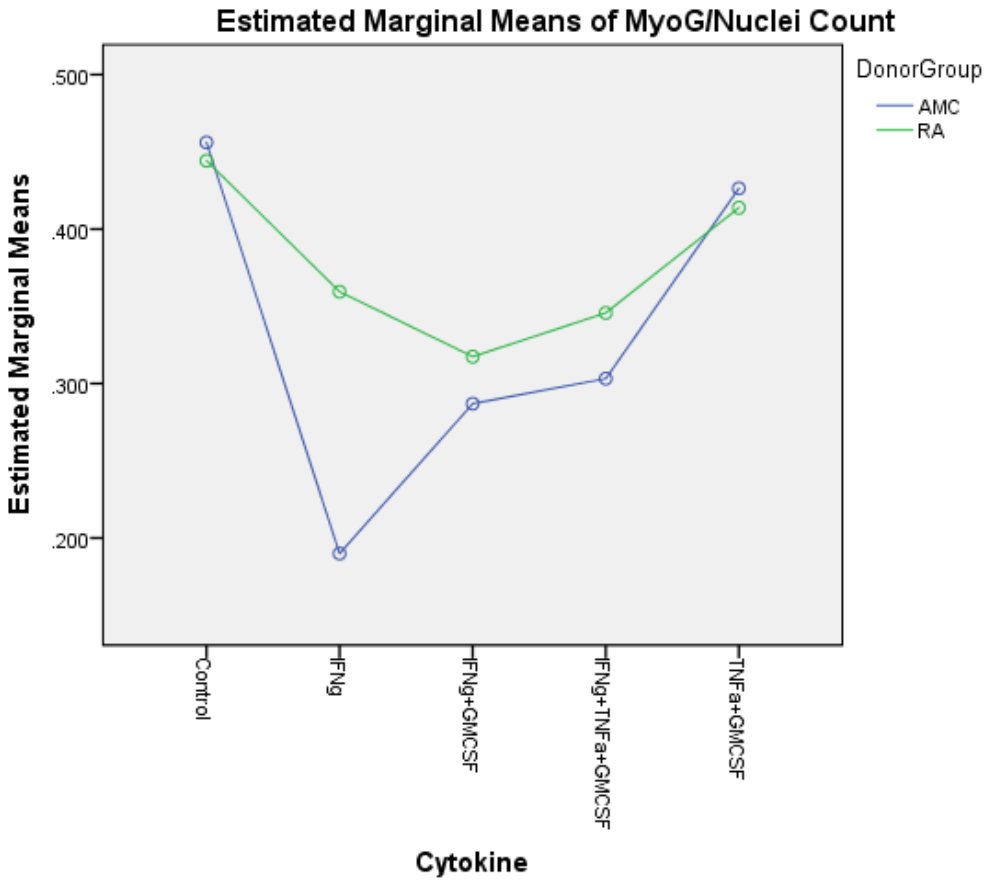

Tests of Between-Subjects Effects

Dependent Variable: SAA+ Area/CS Area

Source	Type III Sum of Squares	df	Mean Square	F	Sig.
Corrected Model	0.010[a]	9	0.001	0.788	0.633
Intercept	1.091	1	1.091	774.128	0.000
Donor Group	0.004	1	0.004	2.730	0.122
Cytokine	0.005	4	0.001	0.847	0.520
Donor Group * Cytokine	0.001	4	0.000	0.111	0.977
Error	0.018	13	0.001		
Total	1.206	23			
Corrected Total	0.028	22			

a. R Squared = 0.353 (Adjusted R Squared = -0.095)

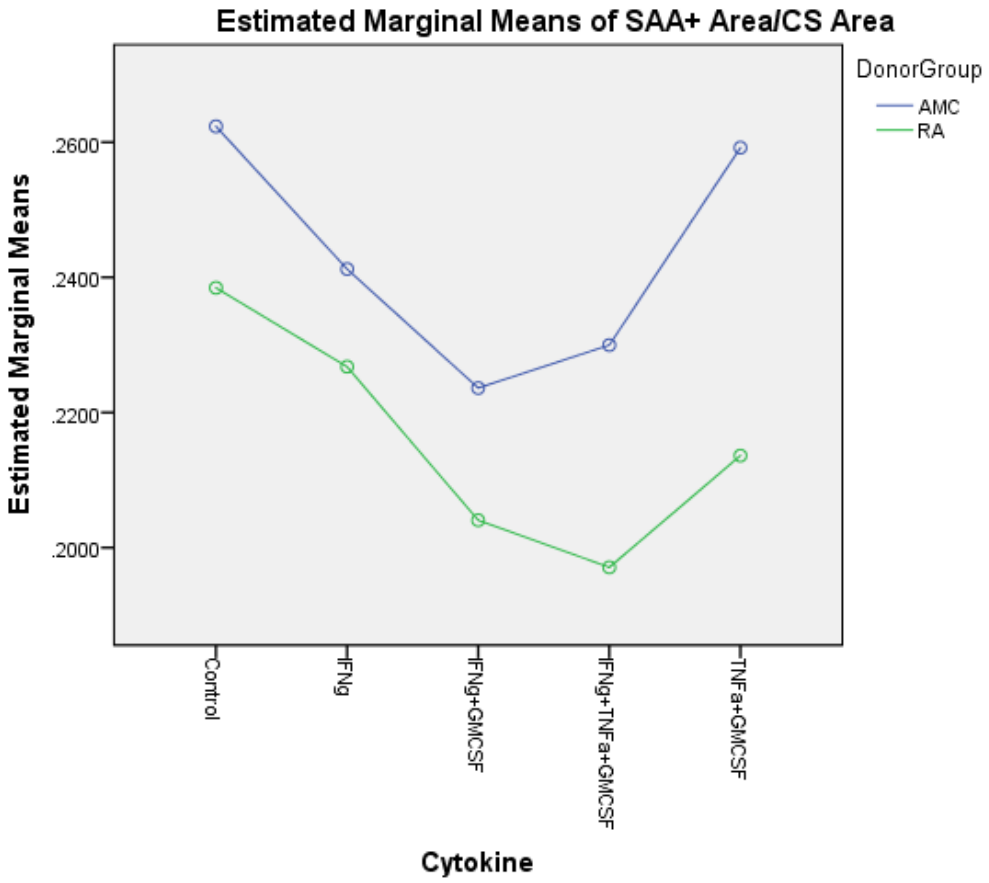

Tests of Between-Subjects Effects

Dependent Variable: Fiber Diameter (µm)

Source	Type III Sum of Squares	df	Mean Square	F	Sig.
Corrected Model	2.785[a]	9	0.309	2.182	0.098
Intercept	3137.905	1	3137.905	22123.639	0.000
Donor Group	0.905	1	0.9eter05	6.383	0.025
Cytokine	1.432	4	0.358	2.525	0.092
Donor Group * Cytokine	0.393	4	0.098	0.694	0.610
Error	1.844	13	0.142		
Total	3530.535	23			
Corrected Total	4.629	22			

a. R Squared = 0.602 (Adjusted R Squared = 0.326)

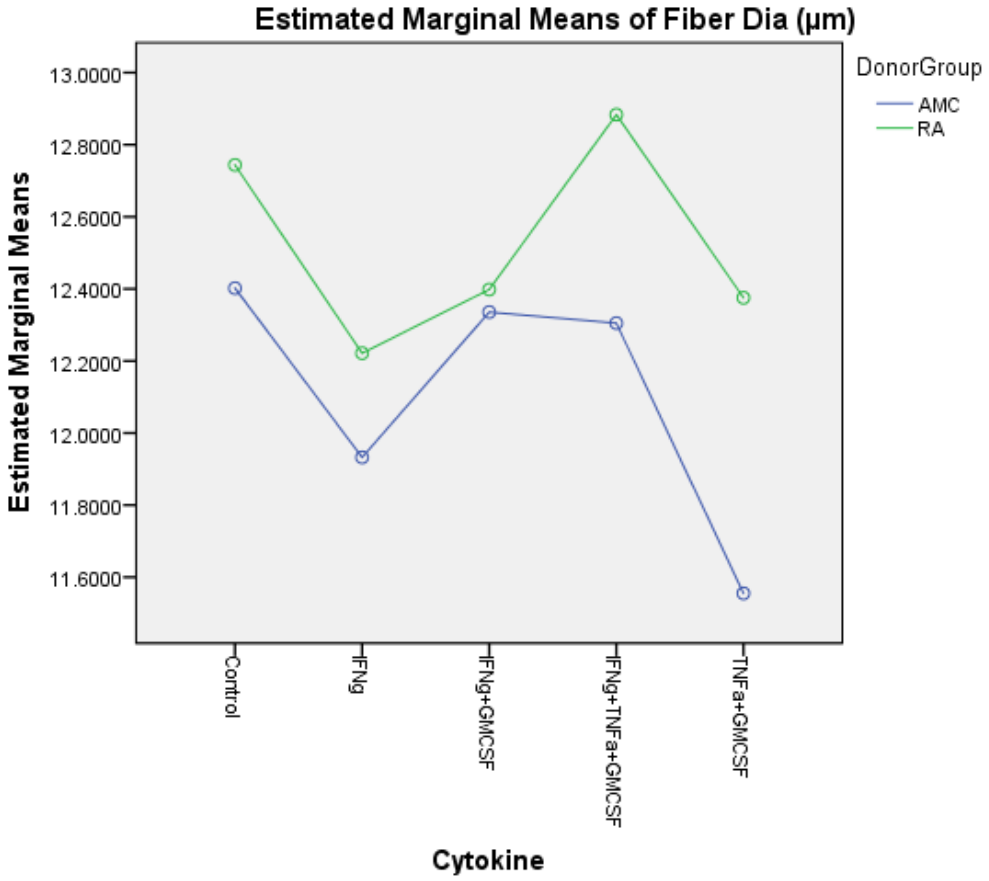

Multiple Comparisons

Dependent Variable: Fiber Diameter (μm)

Tukey HSD

(I) Cytokine	(J) Cytokine	Mean Difference (I-J)	Std. Error	Sig.	95% Confidence Interval	
					Lower Bound	Upper Bound
Control	IFNg	0.482040	0.2750369	0.438	-0.383963	1.348043
	IFNg+GMCSF	0.234008	0.2381890	0.858	-0.515973	0.983989
	IFNg+TNFa+GMCSF	-0.044913	0.2381890	1.000	-0.794894	0.705068
	TNFa+GMCSF	0.559789	0.2381890	0.190	-.190192	1.309770
IFNg	Control	-0.482040	0.2750369	0.438	-1.348043	0.383963
	IFNg+GMCSF	-0.248032	0.2750369	0.891	-1.114036	0.617971
	IFNg+TNFa+GMCSF	-0.526953	0.2750369	0.357	-1.392957	0.339050
	TNFa+GMCSF	0.077749	0.2750369	0.998	-0.788254	0.943753
IFNg+GMCSF	Control	-0.234008	0.2381890	0.858	-0.983989	0.515973
	IFNg	0.248032	0.2750369	0.891	-0.617971	1.114036
	IFNg+TNFa+GMCSF	-0.278921	0.2381890	0.767	-1.028902	0.471060
	TNFa+GMCSF	0.325781	0.2381890	0.657	-0.424199	1.075762
IFNg+TNFa+GMCSF	Control	0.044913	0.2381890	1.000	-0.705068	0.794894
	IFNg	0.526953	0.2750369	0.357	-0.339050	1.392957
	IFNg+GMCSF	0.278921	0.2381890	0.767	-0.471060	1.028902
	TNFa+GMCSF	0.604703	0.2381890	0.141	-0.145278	1.354683
TNFa+GMCSF	Control	-0.559789	0.2381890	0.190	-1.309770	0.190192
	IFNg	-0.077749	0.2750369	0.998	-0.943753	0.788254
	IFNg+GMCSF	-0.325781	0.2381890	0.657	-1.075762	0.424199
	IFNg+TNFa+GMCSF	-0.604703	0.2381890	0.141	-1.354683	0.145278

Based on observed means.

The error term is Mean Square (Error) = 0.142.

Appendix C: Abbreviations

RA	Rheumatoid Arthritis
HSkM	Human skeletal muscle
SAA	Sarcomeric alpha actinin
MyoG	Myogenin
IL	Interleukin
TNF	Tumor Necrosis Factor
IFN	Interferon
TGF	Transforming Growth Factor
GMCSF	Granulocyte Macrophage Colony – Stimulating Factor
CSA	Cross-sectional Area
HLA	Human Leukocyte Antigen
MHC	Major Histocompatibility Complex
RF	Rheumatoid Factor
ACPA	Anti-Citrullinated Protein Antibody
APC	Antigen Presenting Cells
DPBS	Dulbecco's phosphate-buffered saline
AA	Antibiotic-Antimycotic
PBS	Phosphate Buffer Saline
PDMS	Polydimethylsiloxane
ACA	6-Aminocaproic Acid
PFA	Paraformaldehyde
BSA	Bovine Serum Albumin

References

1. Lieber, R.L., *Skeletal Muscle Structure, Function, & Plasticity: The Physiological Basis of Rehabilitation.* 2nd ed. 2002, Baltimore: Lippincott Williams & Wilkins.

2. Martini, Timmons & Tallitsch, *Human Anatomy*, 6th Edition, 2009 Pearson Education, Inc., publishing as Pearson Benjamin Cummings.

3. Kathryn North. *Why is α-Actinin-3 Deficiency So Common in the General Population? The Evolution of Athletic Performance.* Twin Research and Human Genetics 11(4):384-94 · August 2008

4. Thornell, L.E., *Sarcopenic obesity: satellite cells in the aging muscle.* Curr Opin Clin Nutr Metab Care, 2011. 14(1): p. 22-7.

5. Le Grand, F. and M.A. Rudnicki, *Skeletal muscle satellite cells and adult myogenesis*. Curr Opin Cell Biol, 2007. 19(6): p. 628-33.

6. Zammit, P.S., T.A. Partridge, and Z. Yablonka-Reuveni, *The skeletal muscle satellite cell: the stem cell that came in from the cold.* J Histochem Cytochem, 2006. 54(11): p. 1177-91.

7. Charge, S.B. and M.A. Rudnicki, *Cellular and molecular regulation of muscle regeneration.* Physiol Rev, 2004. 84(1): p. 209-38.

8. Delgado, I., et al., *Dynamic gene expression during the onset of myoblast differentiation in vitro.* Genomics, 2003. 82(2): p. 109-21.

9. Venuti, J.M., et al., *Myogenin is required for late but not early aspects of myogenesis during mouse development.* J Cell Biol, 1995. 128(4): p. 563-76.

10. Bazgir B, Fathi R, Rezazadeh Valojerdi M, Mozdziak P, Asgari AR. *Satellite cells contribution to exercise mediated muscle hypertrophy and repair.* Cell J. 2017; 18(4): 473-484.

11. Rothschild BM[1], Turner KR, DeLuca MA. *Symmetrical erosive peripheral polyarthritis in the Late Archaic Period of Alabama.* Science. 1988 Sep 16;241(4872):1498-501.

12 Yinon Shapira, Nancy Agmon-Levin & Yehuda Shoenfeld *Geoepidemiology of autoimmune rheumatic diseases.* Nature Reviews Rheumatology volume 6, pages 468–476 (2010).

13 https://www.globaldata.com/store/report/gdhcer145-16--epicast-report-rheumatoid-arthritis-epidemiology-forecast-to-2025/

14 Lee DM, Weinblatt ME. *Rheumatoid arthritis.* Lancet. 2001 Sep 15;358(9285):903-11.

15 Bottini, N. & Firestein, *Epigenetics in Rheumatoid Arthritis: A Primer for Rheumatologists* G.S. Curr Rheumatol Rep (2013) 15: 372. https://doi.org/10.1007/s11926-013-0372-9

16 Smolen JS, Aletaha D, McInnes IB. *Rheumatoid arthritis*. Lancet. 2016 Oct 22;388(10055):2023-2038. doi: 10.1016/S0140-6736(16)30173-8. Epub 2016 May 3.

17 Selim Nalbant and Ahmet Merih Birlik (February 22nd, 2017). *Cytokines in Rheumatoid Arthritis (RA), New Developments in the Pathogenesis of Rheumatoid Arthritis*, Lazaros I. Sakkas, IntechOpen, DOI: 10.5772/65893. Available from: https://www.intechopen.com/books/new-developments-in-the-pathogenesis-of-rheumatoid-arthritis/cytokines-in-rheumatoid-arthritis-ra-

18 Firestein, G. S. (2017, August 30). *Pathogenesis of Rheumatoid Arthritis.* Retrieved from https://www.uptodate.com/contents/pathogenesis-of-rheumatoid-arthritis

19 Kim M. Huffman, Ryan Jessee, Brian Andonian, Brittany N. Davis, Rachel Narowski, Janet L. Huebner, Virginia B. Kraus, Julie McCracken, Brian F. Gilmore, K. Noelle Tune, Milton Campbell, Timothy R. Koves, Deborah M. Muoio, Monica J. Hubal and William E. Kraus. *Molecular alterations in skeletal muscle in rheumatoid arthritis are related to disease activity, physical inactivity, and disability. Arthritis Research & Therapy* 2017.

20 Brennan FM, Maini RN, Feldmann M. *TNF alpha--a pivotal role in rheumatoid arthritis?* Br J Rheumatol. 1992 May;31(5):293-8.

21 Valencia X, Stephens G, Goldbach-Mansky R, Wilson M, Shevach EM, Lipsky PE. *TNF downmodulates the function of human CD4+CD25hi T-regulatory cells.* Blood. 2006 Jul 1;108(1):253-61. Epub 2006 Mar 14.

22 Catrina AI, af Klint E, Ernestam S, Catrina SB, Makrygiannakis D, Botusan IR, Klareskog L, Ulfgren AK. *Anti-tumor necrosis factor therapy increases synovial osteoprotegerin expression in rheumatoid arthritis* Arthritis Rheum. 2006 Jan;54(1):76-81.

23 Alvaro-Gracia JM, Zvaifler NJ, Firestein GS. *Cytokines in chronic inflammatory arthritis. IV. Granulocyte/macrophage colony-stimulating factor-mediated induction of class II MHC antigen on human monocytes: a possible role in rheumatoid arthritis.* J Exp Med. 1989 Sep 1;170(3):865-75.

24 Burmester GR, Weinblatt ME, McInnes IB, Porter D, Barbarash O, Vatutin M, Szombati I, Esfandiari E, Sleeman MA, Kane CD, Cavet G, Wang B, Godwood A, Magrini F; EARTH Study Group. *Efficacy and safety of mavrilimumab in subjects with rheumatoid arthritis.* Ann Rheum Dis. 2013 Sep 1;72(9):1445-52. doi: 10.1136/annrheumdis-2012-202450. Epub 2012 Dec 12.

25 Behrens F, Tak PP, Ostergaard M, et al. MOR103, *A human monoclonal antibody to granulocyte-macrophage colony-stimulating factor, in the treatment of patients with moderate rheumatoid arthritis: results of a phase Ib/IIa randomised, double-blind, placebo-controlled, dose-escalation trial.* Ann Rheum Dis 2015;74: 1058–1064.

26 Cheng, Cindy S., et al. *Physiology and metabolism of tissue-engineered skeletal muscle.* Experimental Biology and Medicine 239.9 (2014): 1203-1214.

27 Madden, Lauran, et al. *Bioengineered human myobundles mimic clinical responses of skeletal muscle to drugs.* Elife 4 (2015): e04885.

28 Qazi, Taimoor H., et al. *Biomaterials based strategies for skeletal muscle tissue engineering: existing technologies and future trends.* Biomaterials 53 (2015): 502-521.

29 Khodabukus, Alastair, and Keith Baar. *Factors That Affect Tissue-Engineered Skeletal Muscle Function and Physiology.* Cells Tissues Organs 202.3-4 (2016): 159-168.

30 Shadrin, I. Y., A. Khodabukus, and N. Bursac. *Striated muscle function, regeneration, and repair.* Cellular and Molecular Life Sciences 73.22 (2016): 4175-4202.

31 Juhas, Mark, and Nenad Bursac. *Roles of adherent myogenic cells and dynamic culture in engineered muscle function and maintenance of satellite cells.* Biomaterials 35.35 (2014): 9438-9446.